USAAML TECHNICAL REPORT 65-30

CARGO RESTRAINT CONCEPTS FOR CRASH RESISTANCE

Technical Report
AvSER 64-13

By

James P. Avery, Ph. D.

June 1965

U. S. ARMY AVIATION MATERIEL LABORATORIES
FORT EUSTIS, VIRGINIA

CONTRACT DA 44-177-AMC-116(T)

AVIATION SAFETY ENGINEERING AND RESEARCH

DDC Availability Notice

Qualified requesters may obtain copies of this report from DDC.

This report has been furnished to the Department of Commerce for sale to the public.

Disclaimer

The findings in this report are not to be construed as an official Department of the Army position, unless so designated by other authorized documents.

When Government drawings, specifications, or other data are used for any purpose other than in connection with a definitely related Government procurement operation, the United States Government thereby incurs no responsibility nor any obligation whatsoever; and the fact that the Government may have formulated, furnished, or in any way supplied the said drawings, specifications or other data is not to be regarded by implication or otherwise as in any manner licensing the holder or any other person or corporation, or conveying any rights or permission, to manufacture, use, or sell any patented invention that may in any way be related thereto.

Disposition Instructions

Destroy this report when it is no longer needed. Do not return it to the originator.

HEADQUARTERS
U S ARMY TRANSPORTATION RESEARCH COMMAND
FORT EUSTIS, VIRGINIA 23604

The need for a thorough investigation of cargo restraint criteria for helicopters and fixed wing aircraft subjected to survivable crash conditions and the subsequent delineation of design technique and selection of appropriate materials responsive to said criteria provide the basis for this study. This command concurs in the approach used, conclusions drawn, and recommendations made in this report.

This command is continuing its research and exploratory development program and will render recommendations for restraint criteria changes for Army aircraft and accompanying recommendations for restraint systems repponsive to said criteria for the near future. This program has the joint aim of providing maximum crew protection and maximum system operational efficiency.

NOTE

On 1 March 1965, *after this report had been prepared,* the name of this command was changed from U.S. Army Transportation Research Command to:

U.S. ARMY AVIATION MATERIEL LABORATORIES

Task 1A024701A12101
Contract DA 44-177-AMC-116(T)
USAAML Technical Report 65-30
June 1965

CARGO RESTRAINT CONCEPTS

FOR CRASH RESISTANCE

Technical Report
AvSER 64-13

by
James P. Avery, Ph. D.

Prepared by
Aviation Safety Engineering and Research
2641 E. Buckeye Road
Phoenix, Arizona
a Division of
Flight Safety Foundation, Inc.

for
U. S. ARMY AVIATION MATERIEL LABORATORIES
FORT EUSTIS, VIRGINIA

ABSTRACT

This report covers an investigation of three cargo restraint concepts: (1) an extensible-net-type restraint (such as a nylon net) secured directly to the airframe, (2) the same extensible net attached to load limiters (attenuators), and (3) an inextensible-net-type restraint (such as a steel net) attached to load limiters. Each concept was investigated analytically using computer simulation to determine the dynamic performance of the system under the action of crash acceleration pulses. Drop tests were also conducted to verify analyses.

General comparisons were made to obtain the advantages and shortcomings of each straint concept as well as the influence of controllable parameters.

A substudy of the nature of the probable crash induced acceleration pulse was also undertaken. This led to a proposed standard pulse for cargo restraint design purposes.

CONTENTS

CONTENTS (Contd.)

ILLUSTRATIONS

ILLUSTRATIONS (Contd.)

SUMMARY

This report presents the findings of an investigation of several cargo restraint system concepts that appear to be potentially useful in a practical integrated cargo restraint system for cargo transport aircraft. The cargo aircraft considered are the U. S. Army Caribou, a fixed-wing aircraft, and the U. S. Army CH-47A Chinook, a rotary-wing aircraft. A primary criterion was assumed to be the system strength-to-weight ratio; however, other criteria such as simplicity and control of cargo displacement were given consideration.

A preliminary study of the crash induced acceleration pulse that drives a cargo system was first undertaken as fundamental to any analysis of cargo restraint concepts. A survey of available acceleration-time data for aircraft crashes, together with a computer simulation of the gross features of crash dynamics, were employed to arrive at a suitable acceleration pulse for cargo restraint design for the Caribou. The input pulse for the Chinook was assumed to follow the pattern established through controlled crash tests of other helicopters conducted by AvSER.

For the fixed-wing Caribou, three cargo restraint concepts were explored: an extensible-net-type restraint (such as a nylon net) secured to the airframe, an extensible net together with "load limiters" (attenuators), and an inextensible-net-type restraint (such as a steel mesh net) with load limiters. These concepts were investigated analytically, using computer simulation, and experimentally, by means of drop tests, to determine the dynamic response to a standard input acceleration pulse. The behavior characteristics such as relative displacement, load-limiter stroke, and dynamic overshoot were obtained for each concept under various values of the controllable parameters. The performance of each concept was determined and comparisons made. The investigation revealed that all three concepts contain both advantageous features as well as attendant shortcomings. A preliminary comparison has indicated that the load limited inextensible-net concept contains an advantage in both the system weight requirement and the cargo displacement control. However, as tests were conducted under simulated conditions and with improvised hardware, all three concepts would warrant further development and testing.

The helicopter cargo restraint problem was analyzed broadly, and general observations were made. Further tests were indicated in order to obtain more definitive conclusions. Subsequently, a recent test crash of a CH-21 helicopter demonstrated that the current restraint criteria specified in the operation manual for the CH-47 Chinook helicopter could be reduced to those minimums called for in AR 705-35 if load limiters are used in the forward direction (see below).

	CH-47 Operations Manual	AR Minimums
Forward	8 G's	4 G's
Aft	4 G's	2 G's
Lateral	4 G's	1.5 G's
Vertical	4 G's	2 G's

CONCLUSIONS

It is concluded that:

1. A simple symmetric triangular shaped acceleration-time pulse is found to be suitable for the design of cargo restraint systems for the Caribou aircraft.

2. An extensible-net-type restraint secured to the airframe or cargo floor would experience dynamic overshoot with attendant high requirement for system strength.

3. An extensible-net-type restraint with load limiters would experience relatively large cargo displacements, inclusive of both net deformation and load limiter stroke.

4. An inextensible-net-type restraint with load limiters would hold cargo to smaller displacement but would require use of materials of lower strength-to-weight ratio.

5. A trade-off exists between restraint system weight and cargo displacement. This trade-off may be accomplished by varying controllable parameters for each concept. However, the inextensible-net-type restraint with load limiters is found to be most effective for controlling cargo displacement and minimizing weight.

6. A survey of helicopter crash data indicated that a relatively smaller longitudinal impulse occurs than for fixed-wing aircraft. Also, helicopter crash data revealed that large normal accelerations occur during the primary longitudinal pulse, suggesting the possibility of considerable assistance from friction for cargo restraint. In the absence of specific tests, however, it is not certain that friction and flight load tiedown would alone be sufficient for cargo restraint during a crash.

7. Load limiter application to helicopter cargo restraint appears to provide a lightweight practical solution.

RECOMMENDATIONS

It is recommended that:

1. A cargo restraint system for fixed-wing cargo aircraft be required to withstand a floor acceleration pulse of triangular shape* such as that indicated in Figure 9 of this report.

2. The restraint concept of cargo rigidly secured to airframe be avoided for large mass cargo because the dynamic response to the higher frequency oscillations may result in system failure.

3. An engineering design effort be directed toward the practical development of the other restraint concepts investigated with the objective of achieving integrated restraint systems suitable for various classes of cargo.

4. Tests be conducted on full-scale restraint systems to verify strength and displacement performance.

5. A test program be undertaken to determine minimum requirements for helicopter cargo restraint; specifically, to determine whether flight load tiedown restraint, together with floor friction, is sufficient to restrain cargo during a survivable crash; and if not, the required level for load limiters to be used with helicopter cargo.

* For the rigidly secured cargo application only, the higher frequency oscillations should be superimposed upon the basic triangular pulse.

INTRODUCTION

Unrestrained cargo or cargo that has torn loose from its restraints presents a threat to crew survival during an aircraft crash. Injury may result either from a direct blow dealt by flying cargo or by a secondary missile set in motion by cargo impact. Regardless of the nature of the hazard, the task of achieving a crashworthy cargo restraint assumes significance for crew safety.

This report is designed to summarize the findings of an investigation of several concepts of cargo restraint that appear to have potential value in a practical integrated restraint system aboard the U. S. Army Caribou aircraft and the U. S. Army Chinook aircraft. While the objective of cargo restraint of minimum weight has been assumed as the prime criterion, consideration has also been given to the practical requirements of simplicity, space limitations, and cargo displacement.

The scope of the investigation has been limited to crash safety requirements for missions involving only cargo transportation, not the mixed passenger-cargo mission. In view of this limited concern for crew safety, only accidents involving large longitudinal acceleration were of interest. The restraint system (or barrier) was considered to be subjected to large longitudinal forces. Lateral restraint of cargo was not considered to be pertinent to crew safety.

A study of the probable longitudinal pulse shape and intensity for which cargo restraint must be designed has been included as fundamental to the investigation. This study, however, has been restricted to those crashes deemed to be within survivability limits. Accident investigation experience would indicate that Caribou accidents need only be considered up to an impact angle of approximately 30 degrees; larger angles for cargo transports would likely fall into the nonsurvivable range (producing excessive cockpit collapse).

The cargo restraint problem for the fixed-wing aircraft differs appreciably from that for the helicopter. The two have thus been treated separately in the investigation and are dealt with separately in this report.

It may be noted that the fixed-wing cargo problem presents greater physical difficulties and hence has constituted the principle effort in the investigation. This is reflected in the present report which deals largely with fixed-wing aircraft cargo. Some observations and analyses, nevertheless, have been made on the helicopter cargo problem with a recommendation for further experimentation in this area.

CRASH ACCELERATION PULSE

A survey of available acceleration-time data for aircraft crashes (supplemented by elementary dynamic analysis) was used to define probable bounds on the crash pulse shape, intensity, and duration for survivable Caribou accidents.

A potentially survivable accident is understood to be one in which the basic aircraft structure provides a protective "shell" around the occupants (in this case, the crew) and in which deceleration levels do not exceed physiological limits of survivability. Within the scope of the definition, there remain several threats to survivability:

1. Personnel tiedown chain failure.
2. Lethal environment (including the lethal "missile").
3. Postcrash hazard.

Work is in progress within each of these significant areas in an effort to develop the greatest likelihood of survival in a potentially survivable accident.

In this study, attention is focused upon the specific threat of the lethal missile in the form of dislodged cargo. As noted earlier in this report, the longitudinal acceleration component is the significant component governing the "cargo missile" threat to the crew. Hence, only longitudinal accelerations have been investigated when considering the Caribou. Displayed in Figures 1 through 8 are several typical longitudinal acceleration-time plots for aircraft subjected to controlled crash conditions. A study of references noted on each plot indicates that these controlled crashes fall generally into the survivable range as defined earlier and, hence, represent a reasonable basis for a design criterion. Although specific crash data on the Caribou aircraft (CV-2A, CV-2B, and CV-7A) are lacking, the curves shown are considered typical of what might be expected for the Caribou. (The higher frequency oscillations have been omitted for the sake of clarity in all but Figure 8.)

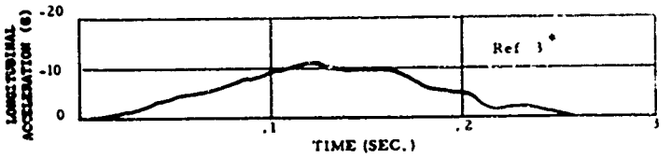

Figure 1. C-46 Controlled Crash Conditions.
Angle of Impact, 15°; Impact Speed, 93 mph.

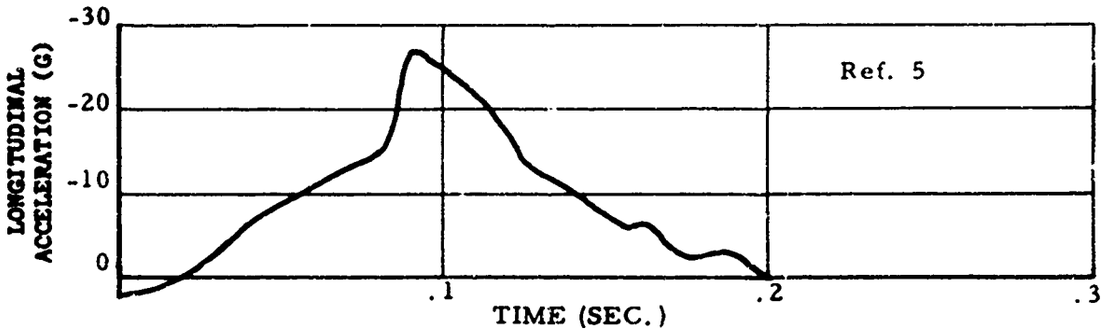

Figure 2. FH-1 Navy Fighter Controlled Crash Conditions.
Angle of Impact, 22°; Impact Speed, 112 mph.

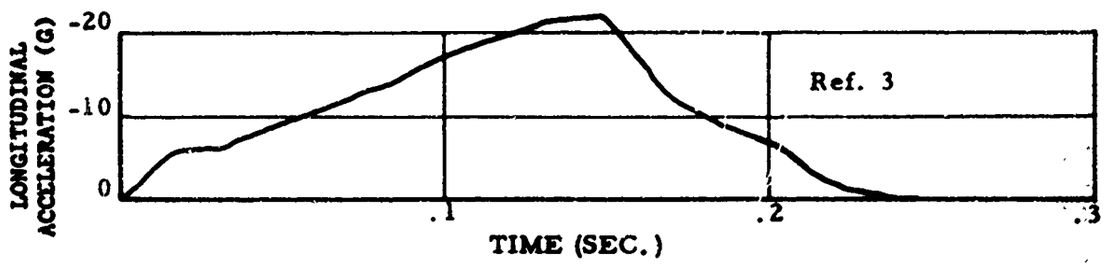

Figure 3. C-46 Controlled Crash Conditions.
Angle of Impact, 29°; Impact Speed, 97 mph.

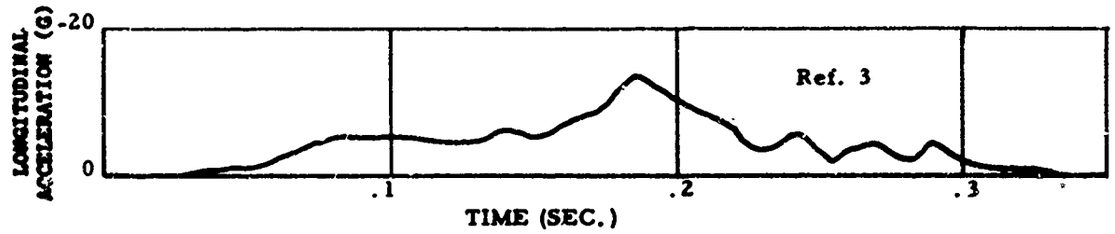

Figure 4. Lodestar Controlled Crash Conditions.
Angle of Impact, 16°; Impact Speed, 109 mph.

* Numbers refer to references listed in reference section.

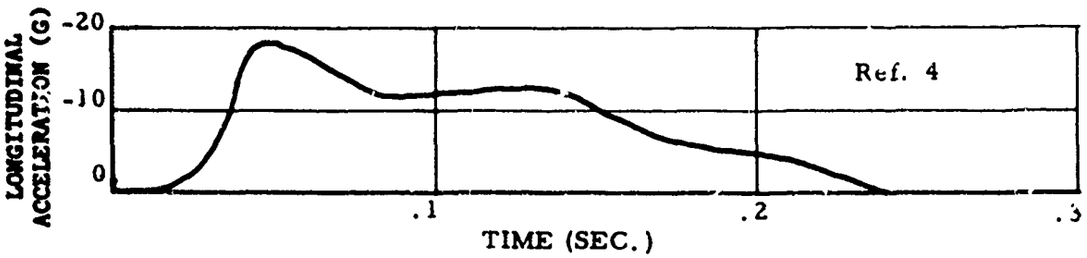

Figure 5. Piper J-3 Controlled Crash Conditions.
Angle of Impact, 60°; Impact Speed, 42 mph.

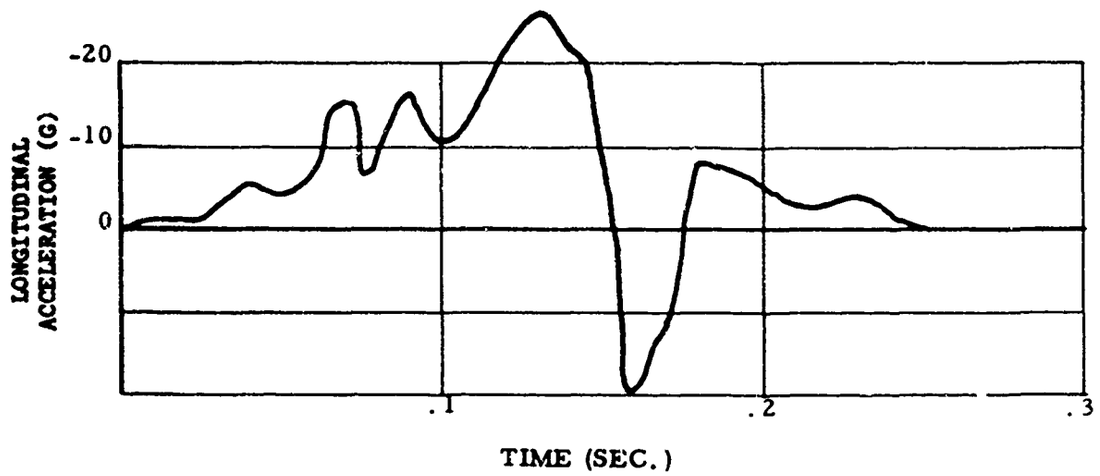

Figure 6. C-45 Controlled Crash Conditions.
Angle of Impact, 40°; Impact Speed, 57 mph.

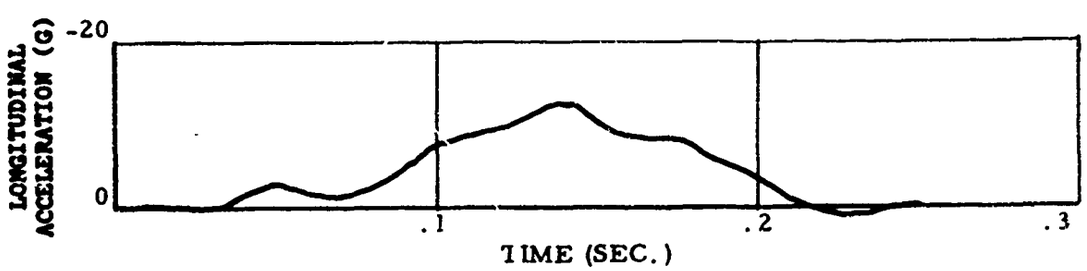

Figure 7. DC-7 Controlled Crash Conditions. (First Impact).
Angle of Impact, 7°; Impact Speed, 153 mph.

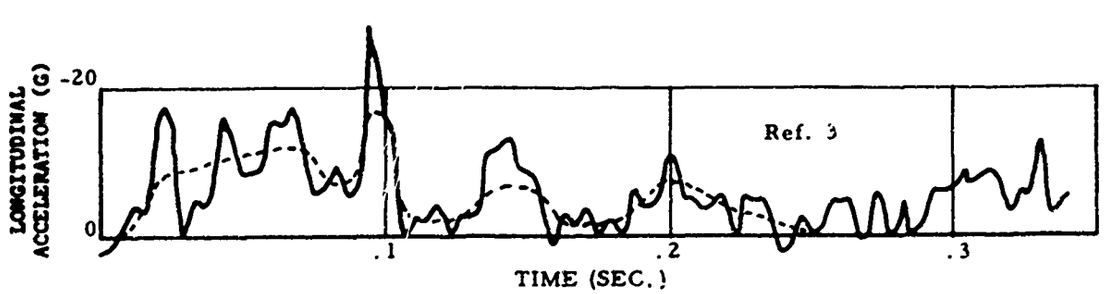

Figure 8. C-82 Controlled Crash Conditions.
Angle of Impact, 16°; Impact Speed, 91 mph.

It may be observed that during the primary impact, the crash pulse is essentially triangular or sinusoidal in shape for each of the above crashes. The "buildup" in deceleration would result from an increased resistance in the longitudinal direction as the aircraft penetrates the soil and as the "structure-collapse-front" moves aft to larger cross-sectional areas. The "falloff" in deceleration can be attributed to the reduced resistance to collapse in post-buckling behavior; additionally, the reduced soil reaction during the spring-back phase, together with a rotation of the longitudinal axis of the aircraft, would contribute to the "falloff". (This becomes apparent in a study of the results of the computer crash pulse simulation discussed later in the report). Consequently, a triangular-shaped pulse is assumed as reasonable for a design pulse. (The effect of pulse shape changes upon restraint system performance is considered later in this report.)

The pulse durations for the crashes surveyed range from a nominal .2 second to approximately .35 second. It should be noted that this parameter would depend largely upon the soil conditions, impact velocity, and impact angle. The softer soils and smaller impact angles would lead to longer pulse duration for a given velocity. A conservative design pulse criterion would be based upon the shortest duration, that is, the steepest impact angle and hardest soil consistent with the limits of survivability.

The maximum intensity of acceleration during the crash pulse is found to vary considerably; however, it is observed to be related to the impact velocity and pulse duration. The area under the acceleration-time curve should approximately equal the net velocity change during the impact. To the extent that rotation of the longitudinal axis occurs during the impact, however, the area under the acceleration-time curve is found to be less than the observed velocity change. This phenomenon is noted in the displayed curves.

A further feature of actual acceleration-time curves is the presence of higher frequency oscillations superimposed upon the basic pulse. This is shown in acceleration-time plot for the C-82, Figure 8, in which the high frequency oscillations were not omitted. It is demonstrated later in this report that these short duration disturbances (including isolated "spikes") have a minor effect upon the performance of a practical cargo restraint system.

A computer simulation of the gross features of crash dynamics is discussed in detail in Appendix I. Such a simulator accepts stiffness constants as input for an assumed nonlinear function for normal ground

reaction force in terms of the interference between the aircraft contour and the ground surface. This force would actually depend upon both the crush strength of the airframe and the resistance modulus of the soil; however, for gross behavior the stiffness constants selected treat soil and structure stiffness inseparably. Also included as input are the impact velocity, the impact angle, the aircraft mass and contour, and a "coefficient of plowing" (an equivalent coefficient of friction). By varying the input parameters within plausible bounds an array of acceleration-time curves for the Caribou has resulted. (See Figures 10A and 10B.)

It is noted that for the various input values selected, the resulting acceleration-time curves agree in essential features with the acceleration-time curves recorded for the actual crash tests. Consequently, the computer simulated pulses, together with the experimental data, appear to form a valid basis for a design pulse or pulses.

In view of the unpredictable nature of accident parameters, a pulse of maximum intensity is suggested as an operating expedient for design purposes. While this is admittedly more severe than the crash pulses likely to be experienced in most survivable Caribou accidents, in the absence of actual test data for the specific aircraft, a conservative design pulse appears justified. Thus, the selected design pulse is as illustrated in Figure 9.

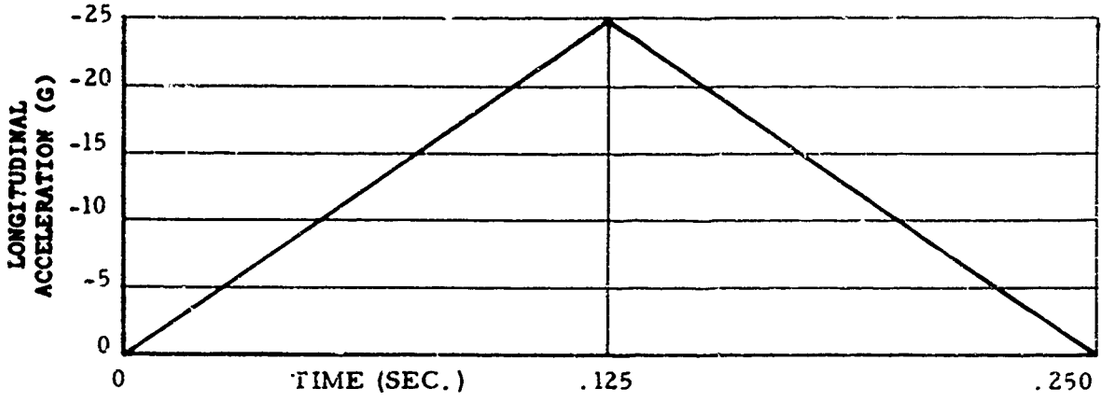

Figure 9. Proposed Design Pulse.

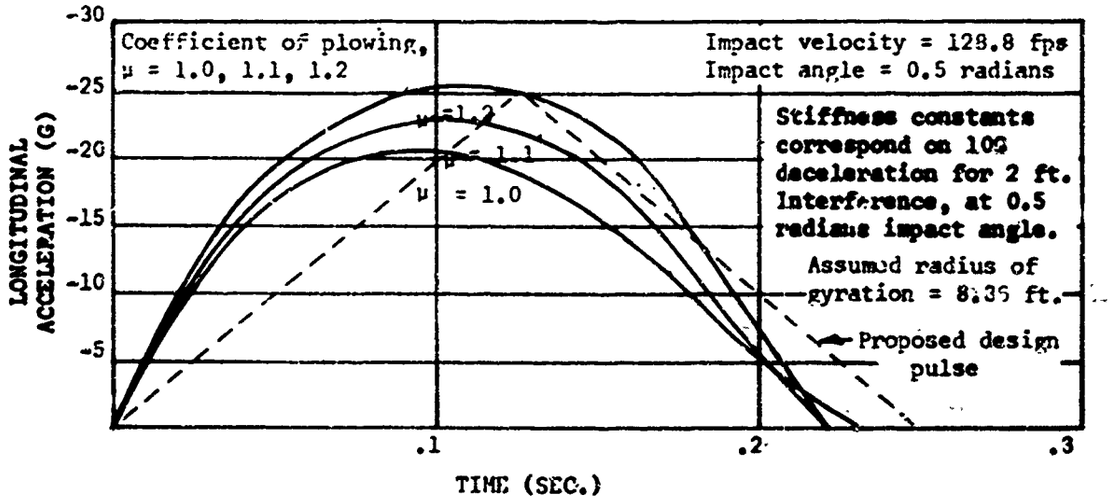

Figure 10A. Simulated Crash Pulses for the Caribou.

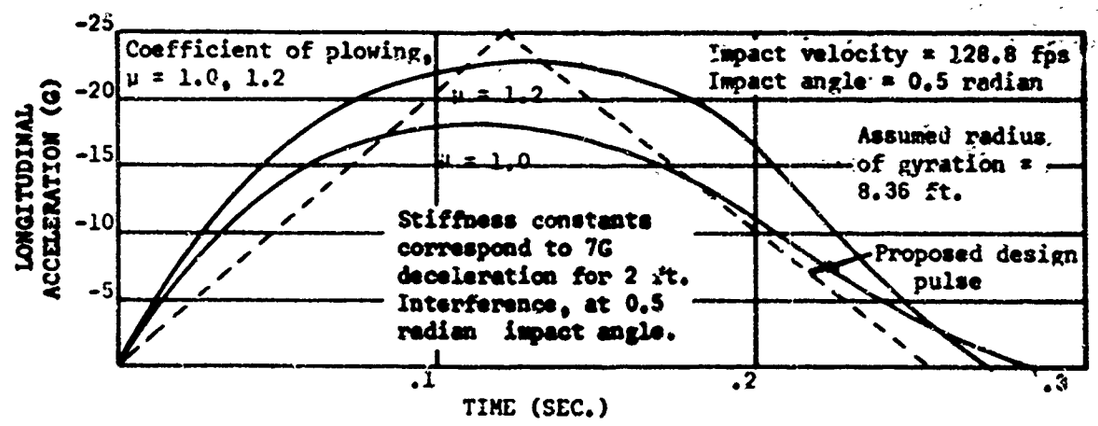

Figure 10B. Simulated Crash Pulses for the Caribou.

CARGO RESTRAINT CONCEPTS

Several design concepts for retaining cargo during a crash situation have been explored in this investigation. These may be described in general terms as follows: (1) direct restraint by rigidly securing the cargo to basic airframe or cargo floor, (2) an extensible-net-type restraint (nylon net, for example) secured to airframe or cargo floor, (3) an extensible net with attachment to airframe through load limiters (energy absorbers), and (4) an inextensible net or barrier (such as a steel mesh net) attached to airframe through load limiters. Each of these concepts has advantageous features as well as attendant shortcomings as will be made evident in further discussion. The following sections contain the detailed discussions for each of the cargo restraint concepts.

RIGID RESTRAINT

A cargo rigidly secured to the airframe would experience the same kinematics as do the points of attachment. Consequently, the restraint strength must at least be sufficient to accommodate the maximum acceleration experienced by the aircraft. Moreover, as true rigidity can never be achieved since some elastic behavior must always be present, the "rigid" restraint system actually constitutes a spring-mass system of large spring constant. As such, it may be responsive to the high frequency oscillations observed to be present in the input acceleration pulse. Due to the unpredictable nature of these high frequency inputs, a sizeable factor-of-safety must be placed upon a rigid restraint design. Otherwise, failure could readily occur at a weak link in the tiedown chain. It is not suggested here that the rigid tiedown concept be avoided in all circumstances, but rather that it does not appear to be practical for securing the larger masses.

EXTENSIBLE NET SECURED TO AIRFRAME

An extensible net secured to the airframe will experience the phenomenon of dynamic overshoot. A time lag occurs (by virtue of the extensibility of the net) between the aircraft deceleration and the cargo deceleration. Consequently, to produce the same total velocity change during impact for cargo and aircraft, the cargo must undergo a greater deceleration in the final stages. This is demonstrated clearly in both the drop tests and the computer simulation of this restraint concept.

Reference is made to Appendix II in which the drop test setup is described in detail and to Appendix III in which the computer simulator for restraint system behavior is discussed.

The extensible net has as desirable features (1) simplicity, a minimum of attendant hardware, (2) relatively high static strength-to-weight ratio, and (3) ability to adapt to various sizes and shapes of cargo. Also present are inherent disadvantages: (1) a high-strength requirement to accommodate dynamic overshoot, and (2) possible large cargo displacement arising from extensibility and dynamic overshoot.

The behavior of a cargo net of extensible type (secured to airframe) is demonstrated by drop test sequence photographs shown in Figure 12 (Test 11). The measured accelerations of both cage (representing aircraft) and cargo, as well as other significant test data, are shown in Figure 11.

Extensible Net Drop Test (No. 11)

Drop Height - 6 ft. free fall

Total cargo relative displacement - 8 in.

Stopping distance of cage - 6 in.

Maximum cage acceleration - 21.5G

Maximum cargo acceleration - 25.6G

Dynamic overshoot factor - 1.19

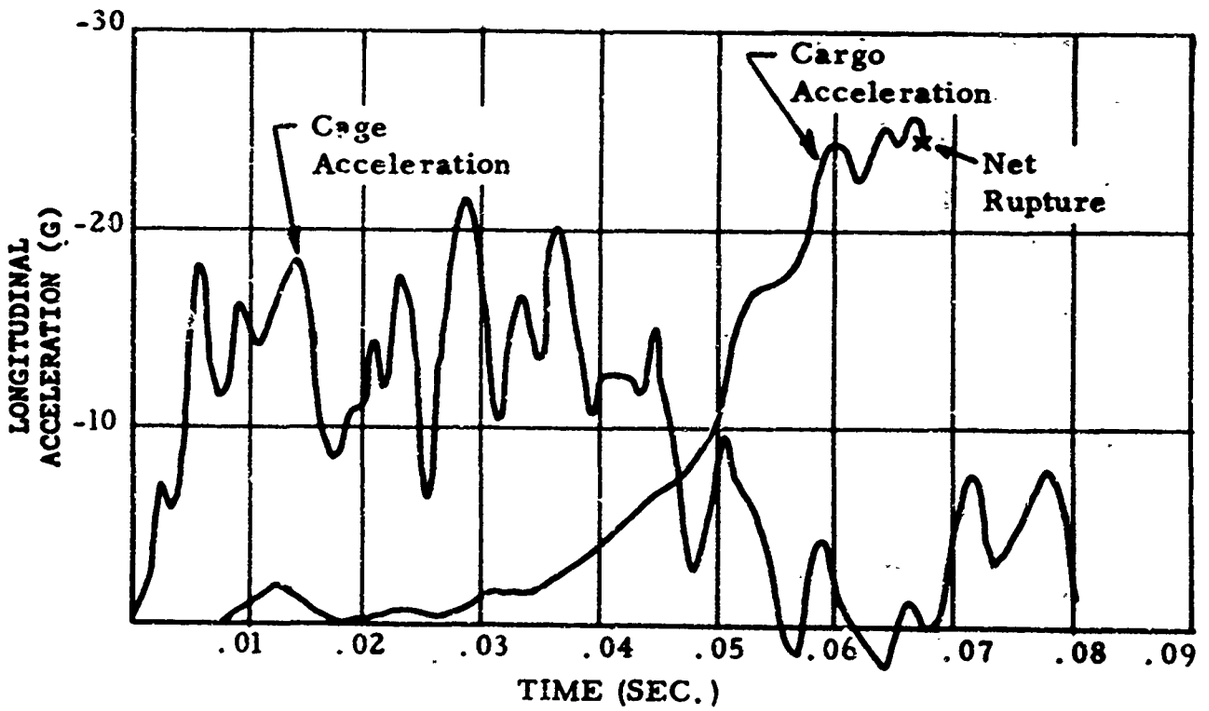

Figure 11. Drop Test 11 Data.

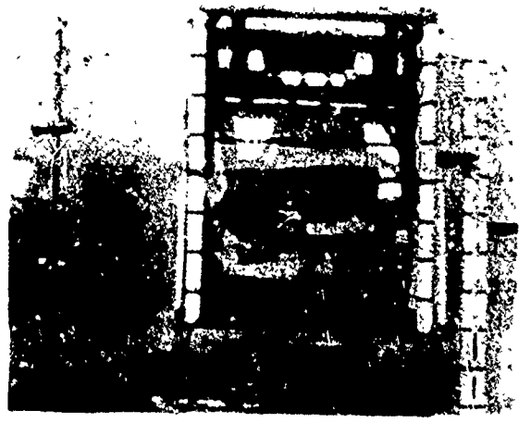

Free Fall

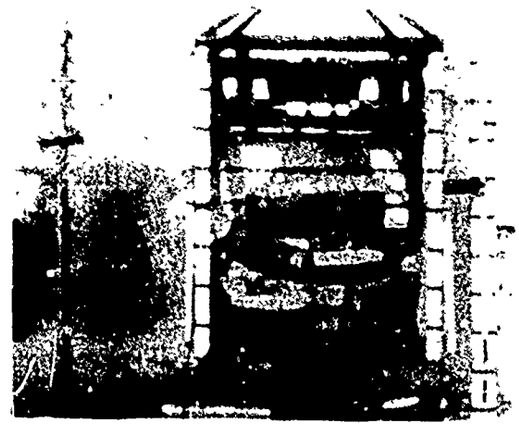

Cage Contacts Honeycomb
Time: 0

Cargo Relative Motion Commences
Time: .021 sec.

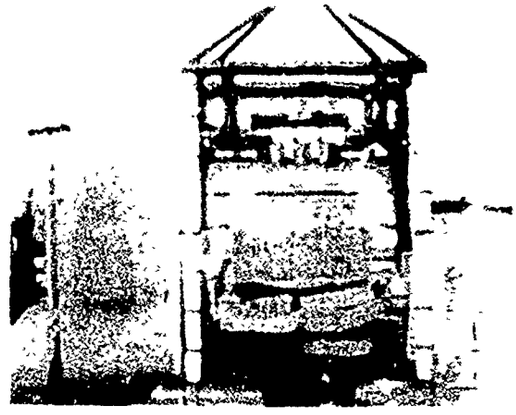

Cage Motion Stops
Time: .043 sec.

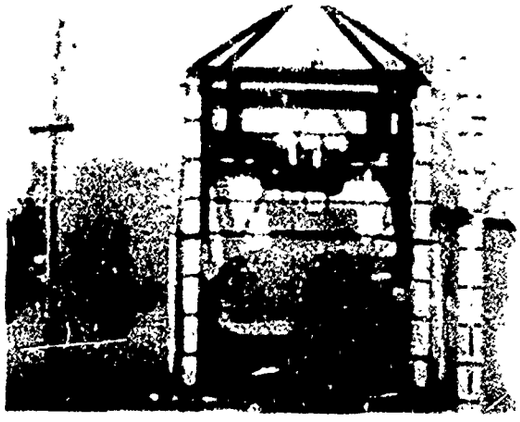

Max Deflection Prior to Rupture
Time: .060 sec.

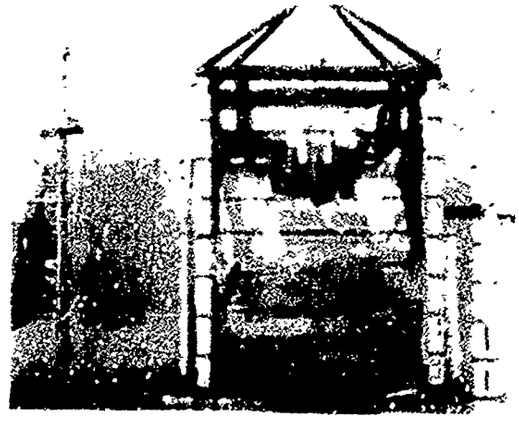

Net Ruptures
Time: .070 sec.

Figure 12. Drop Test 11 Sequence Photos.

Of interest is a computer simulation of this drop test. The measured cage acceleration was employed as the input pulse for the computer. The comparative results are:

	Computer Simulator Results	Drop Test Results
Cage stopping distance	5.96 in.	6 in.
Max. cargo acceleration	-38.8 G	-25.6 G (at rupture)
Max. cargo relative displacement	8.10 in.	8 in.

As the computer simulator does not provide for a cargo net failure, the computer value of maximum cargo acceleration exceeds the acceleration measured in the drop tests, the latter naturally limited by the net rupture. The cargo relative displacement of the simulator should then also be expected to exceed the corresponding test displacement (for the same reason); however, a compensating test feature negated this. Some slip occurred at the nylon net connection to the frame, thus exaggerating test displacements. The simulator and test do agree, however, in the essential cage and cargo behavior.

We conclude that in order to avoid net failure in this test, the net strength would have had to accommodate 39G's and the attendant cargo displacement would have been 8.10 inches.

In the practical Caribou application, a cargo net might be employed in any of several arrangements. It was not considered within the scope of this investigation to explore all such arrangements, but rather to select a representative net arrangement for analysis. For this purpose, a net spanning the cross section of the fuselage is taken with a 2665-pound utility truck as a representative cargo to be restrained. Input data associated with this system was employed for computer simulation leading to results discussed in the following paragraphs.

Plots of cargo net stiffness versus cargo displacement and dynamic overshoot factor versus net stiffness shown in Figure 13 were obtained from computer simulation using various strength nylon nets (and hence various stiffness nylon nets) subjected to the standard cargo mass under a standard input pulse. (The standard pulse selected is intended to serve as a basis for comparison, not as a design criterion.)

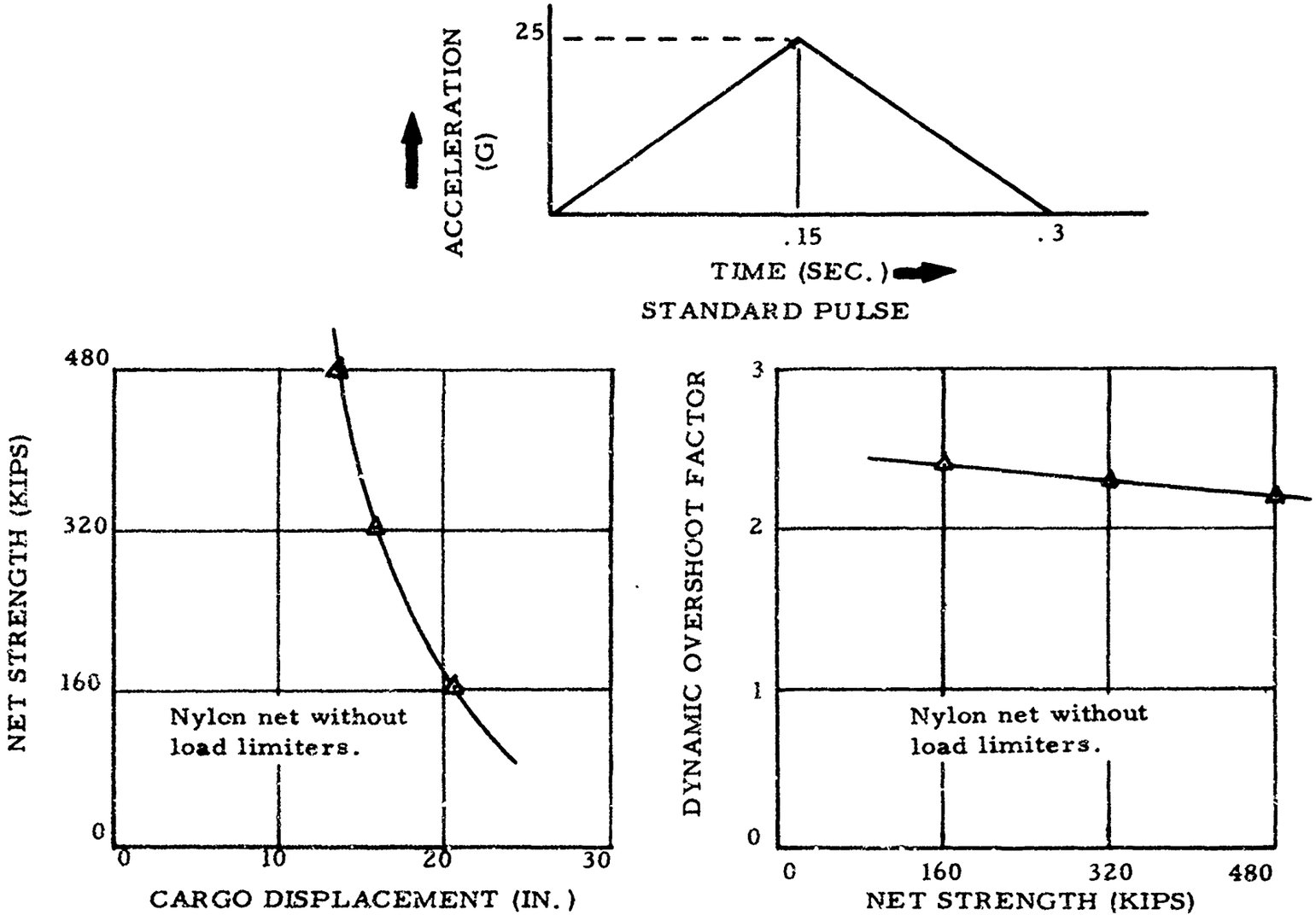

Figure 13 . Cargo Net Stiffness vs. Cargo Displacement and Dynamic Overshoot Factor vs. Net Stiffness.

It is seen that the total displacement of the cargo may be reduced by increasing net stiffness, but at considerable expense in net stiffness (and consequent weight) for small improvements in cargo displacement. Also the dynamic overshoot factors are quite large, ranging from 2.2 to 2.4.

EXTENSIBLE NET WITH LOAD LIMITERS

If an extensible net is secured to the airframe in such a manner that the decelerative forces are transmitted through load limiters, then the maximum acceleration the cargo may experience is determined by the load limiter slip force. A load limiter is understood to mean a device capable of preventing relative displacement for transmitted forces below a specified level (slip force) and allowing displacement at this force level (thus preventing the transmitted force from exceeding the slip force). Consequently, for a given mass attached to a load limiter, the load limiter may be considered an acceleration limiter. In the ensuing discussion, load limiter settings will be specified at G levels for the cargo acceleration. With load limiters used, the phenomenon of dynamic overshoot does not occur.

The advantages of a load limited extensible-net arrangement are: (1) no large forces from dynamic overshoot, hence lighter tiedown hardware and net, and (2) adaptability to many sizes and weights of cargo. The associated shortcomings appear to be (1) increased cargo displacement relative to the aircraft and (2) need for additional hardware, the load limiter devices.

The behavior of a load limited extensible-net-type restraint system is illustrated in drop test No. 10. Sequence photographs and pertinent data are shown in Figures 14 and 15. A computer simulation of this drop test, employing the cage accelerometer data for pulse input, yields the following results:

	Computer Simulated Results	Drop Test Results
Cage stopping distance	5.82 in.	6 in.
Total relative displacement of cargo	15.4 in.	15 in.
Stroke of load limiters	10.5 in.	7 in.
Cargo acceleration	-8 G	-20.2G (max) - 8 G (mean)

Free Fall

Cage Contacts Honeycomb
Time: 0

Cargo Relative Motion Begins
Time: .031 sec.

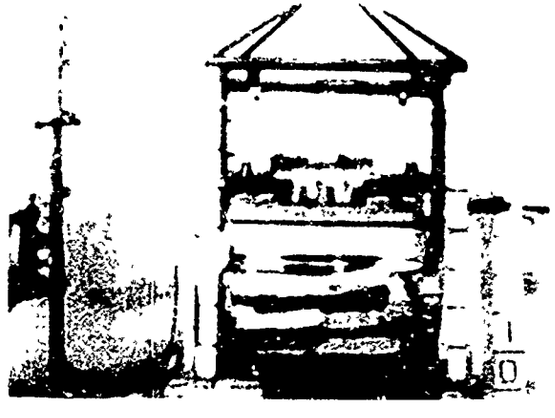

Cage Stops at 6 in. Max. Displ.
Time: .047 sec.

Cargo Relative Motion Begins
Time: .031 sec.

Cage Stops at 6 in. Max. Displ.
Time: .047 sec.

Cargo Rel. Displ. Reaches
Maximum Value
Time: .058 sec.

Load Limiters Commence
Stroking
Time: .062 sec.

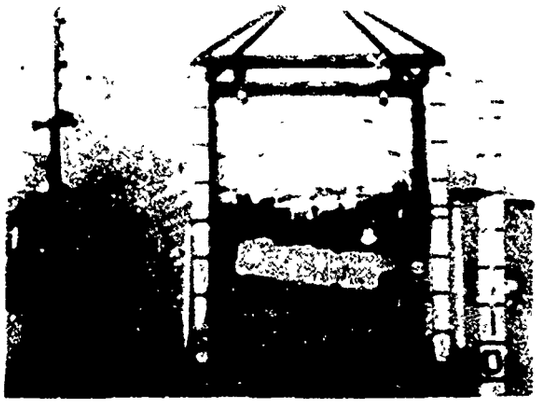

Time: .095 sec.

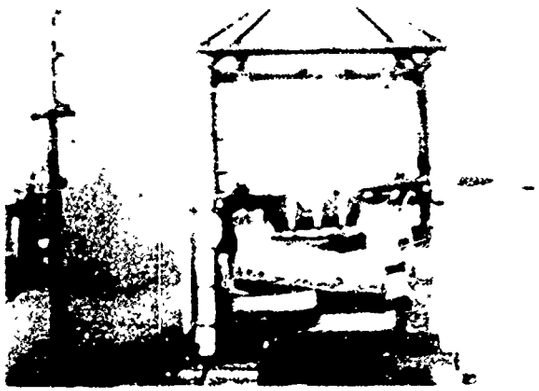

Final Position
Time: .142 sec.

Figure 14. Drop Test 10 Sequence Photos.

Load Limited Extensible Net Drop Test (No. 10)

Drop height - 6 ft. free fall

Total cargo
relative displacement - 15 in.

Stopping distance
of cage - 6 in.

Maximum cage
acc leration - 22.2G

Maximum cargo
acceleration - 20.2G

Mean cargo
acceleration - 8G

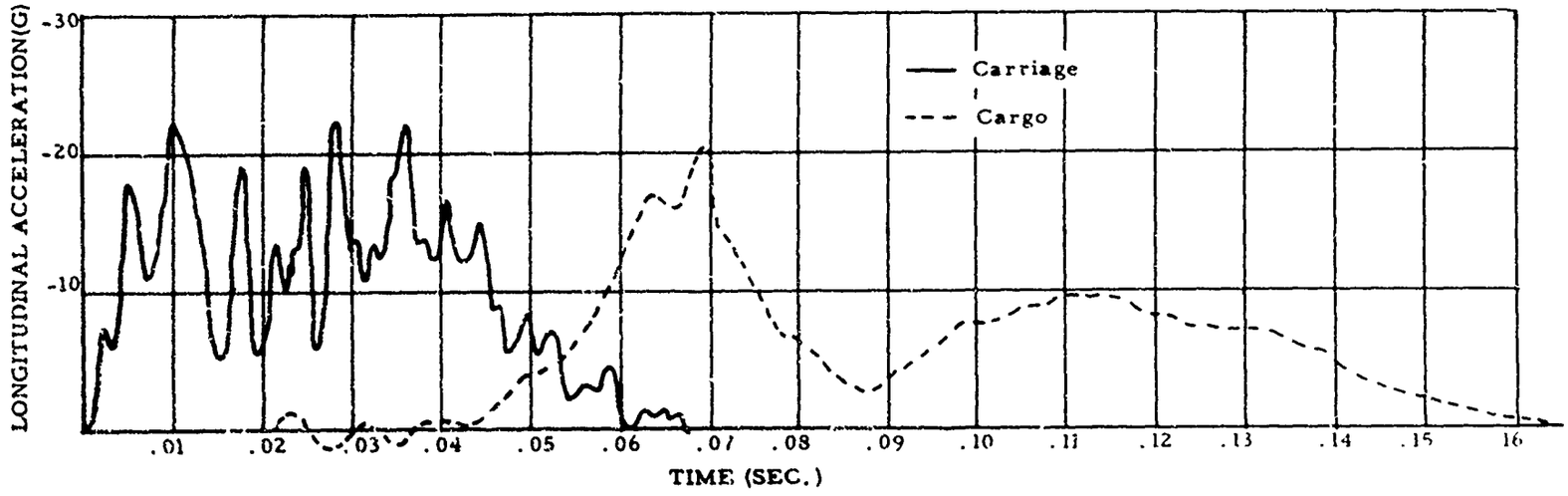

Figure 15. Drop Test 10 Data.

The disparity between test data and simulator data results from two inherent shortcomings in the test procedure. The intermediate sliding frame (to which the net was attached) has a significant mass, permitting an oscillation of cargo relative to the sliding frame (not simulated in the computer program). Thus, the test cargo experienced additional accelerations beyond the load limiter setting. Also the means of attaching the nylon net to the frame permitted a moderate slippage at the attachments. The consequent effect was to increase cargo deflection relative to sliding frame at the expense of load limiter stroke for the drop tests. The resulting total deflection, however, appears to be about the same as that predicted by the computer.

In the application of the load limited extensible net concept to the Caribou cargo retention system, a representative system for purpose of analysis, a net spanning the fuselage cross section retaining a 2665-pound utility truck is taken, with the net attached to the airframe through load limiters. The strength of the net in all cases is assumed to be 1.2 times that required to actuate the load limiters (1.2 taken as a factor of safety).

A plot of load-limiter levels versus total cargo displacement was obtained from computer simulation using the appropriate strength nylon net for each load-limiter level.

It may be observed that cargo displacement is a sensitive function of load limiter level. A modest increase in load limiter level significantly reduces cargo displacement. It should be noted, however, that with increased load limiter level, greater net strength and attendant hardware strength are required. An optimum load limiter level exists between either extreme.

INEXTENSIBLE NET (OR LINKAGE) WITH LOAD LIMITERS

An inextensible-net load-limiter restraint system is understood to include a restraint linkage (such as steel net, chain, membrane, or rigid pallet) in which any deformation in the linkage produces negligible cargo displacement; hence, all displacement occurs at the load limiters through which the restraint forces are transmitted.

As with the extensible load-limiter concept, again dynamic overshoot is not involved; the maximum cargo acceleration is determined simply by the load-limiter level.

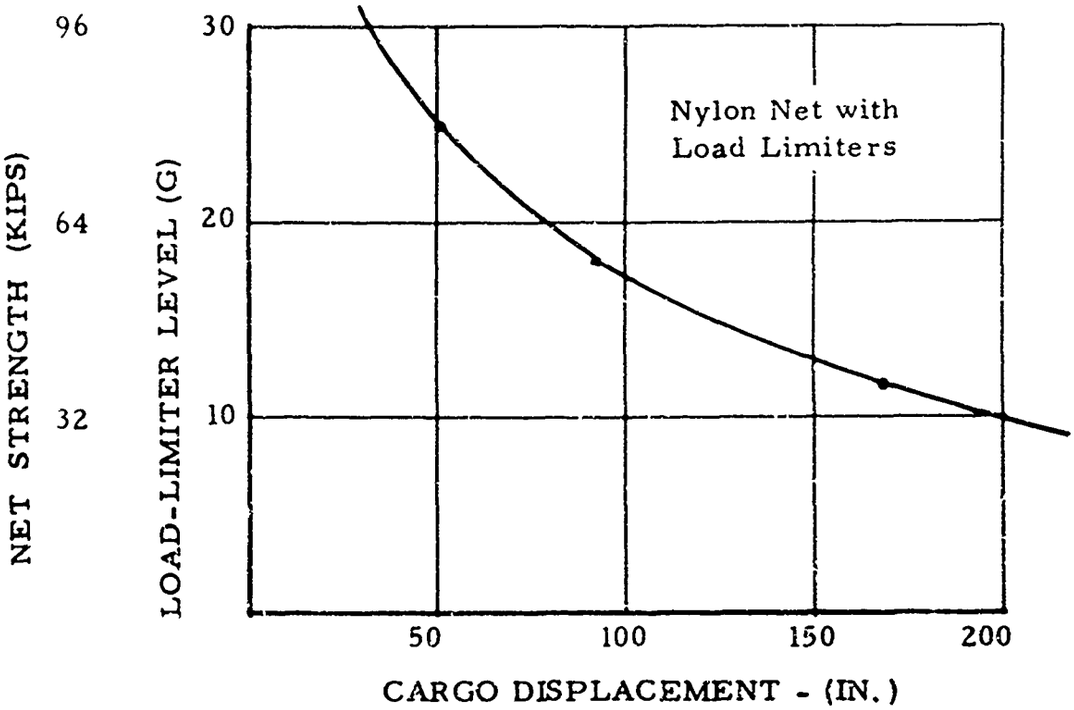

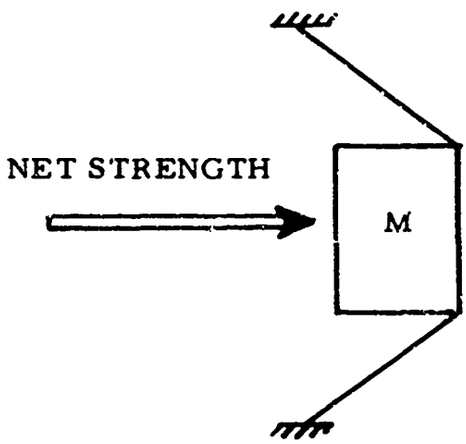

The net strength is defined as the inertia load which would cause rupture of the net (safety factor of 1.2 included).

Figure 16. Cargo Net Strength vs. Cargo Displacement. (Using Load Limiters)

Drop Tests 13 and 14 served to demonstrate the behavior of the load limited inextensible-net concept. In test 13, the load limiter level was set at a low value of approximately 5G and a steel foil membrane (.002-inch-thick) was employed as the cargo net. The experimental results are shown in Figures 17 and 18.

The test simulated on the computer agrees in essential features with the drop test experiment.

	Computer Simulator Results	Drop Test Results
Load-limiter stroke	16.17 in.	12 in. (stopped by protective paper honeycomb)
Max. floor displacement	5.50 in.	6 in.
Cargo acceleration	-5G	-5G (mean value)

Drop test 14 employed stainless steel wire as a restraint net and load limiters set at approximately 8G. Test results are shown in Figures 19 and 20.

The computer simulation of drop test 14 agrees substantially with experimental results.

	Computer Simulator Results	Drop Test Results
Stroke	11.13 in.	9.65 (average)
Max. floor displacement	5.43 in.	6 in.
Cargo acceleration	-8G	-8G(approx. mean)

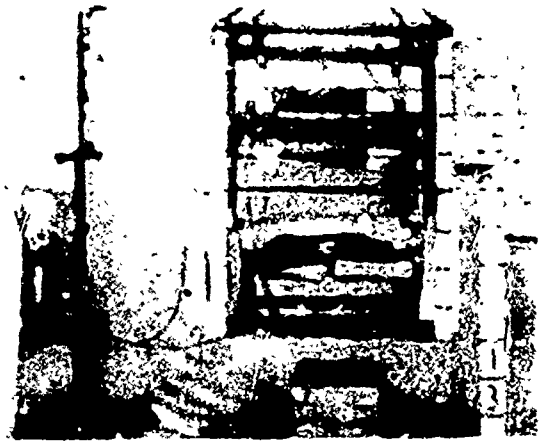

Free Fall

Contact
Time: 0

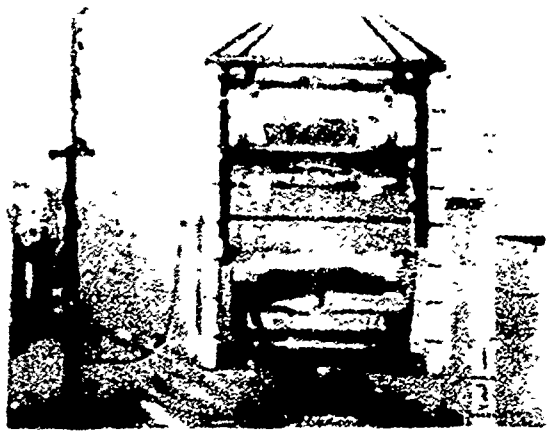

Load Limiters Stroking
Time: .014 sec.

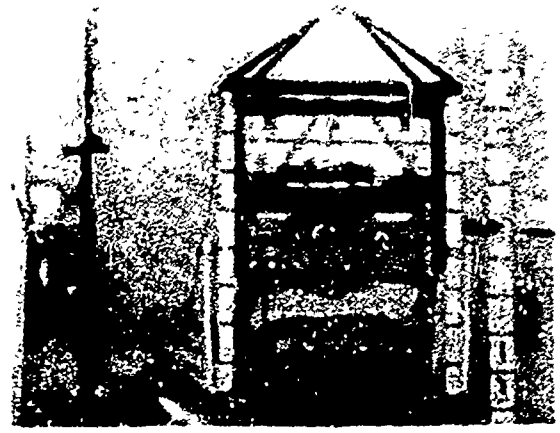

Cage Stops
Time: .031 sec.

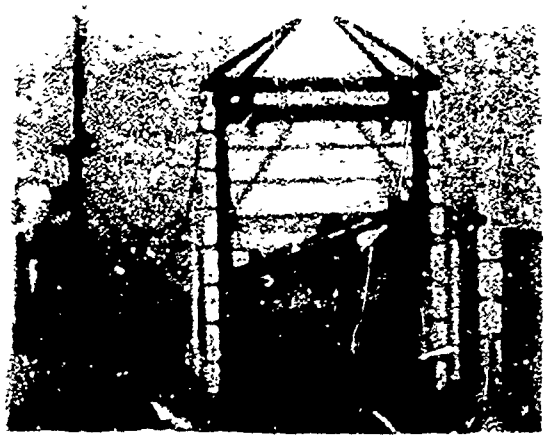

Cargo Stops
Time: .130 sec.

Figure 17. Test 13 Sequence Photos.

Inextensible Net with Load Limiting (No. 13)

Drop height - 6 ft. free fall

Maximum relative cargo displacement - 12 in.

Stopping distance of cage - 6 in.

Maximum cage acceleration - 25.1G

Maximum cargo acceleration - 18.3G

Mean cargo acceleration - 5G

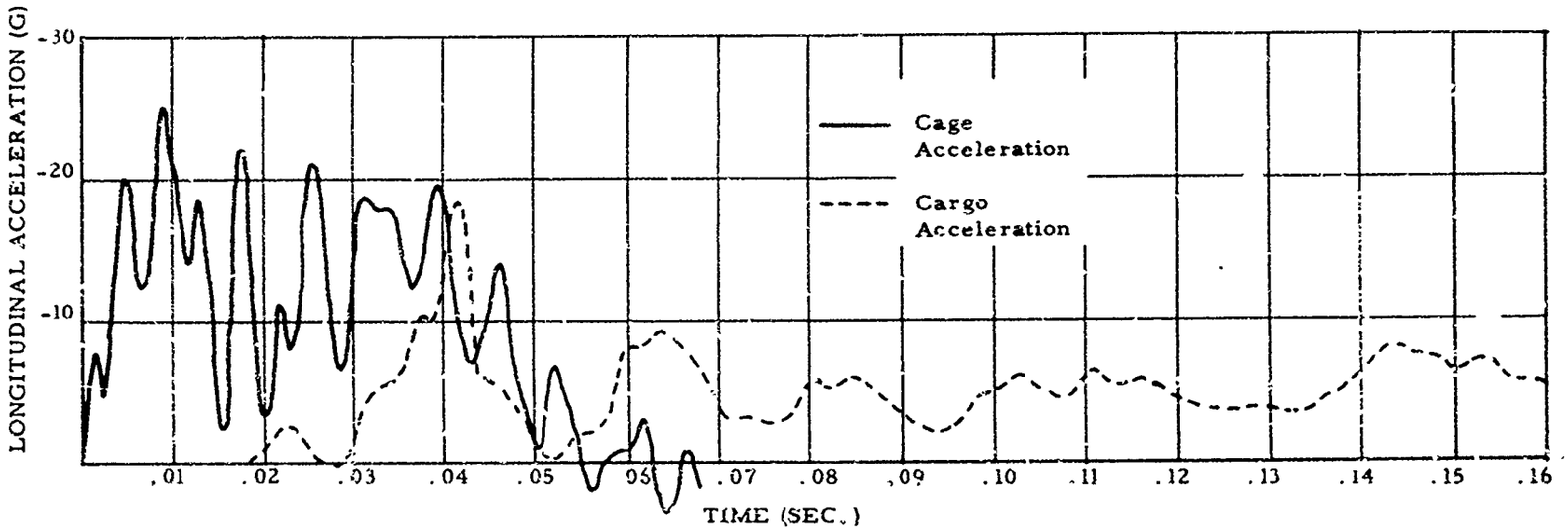

Figure 18. Drop Test 13 Data.

Free Fall

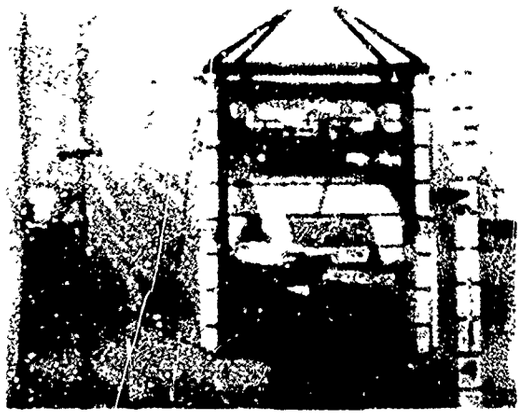

Contact
Time: 0

Load Limiters Commence Stroking
Time: .006 sec.

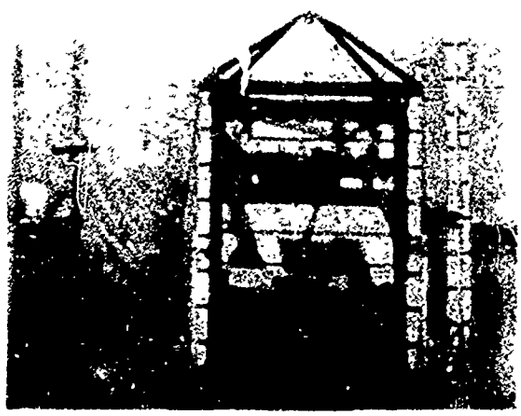

Time: .016 sec.

Cage Stops
Time: .025 sec.

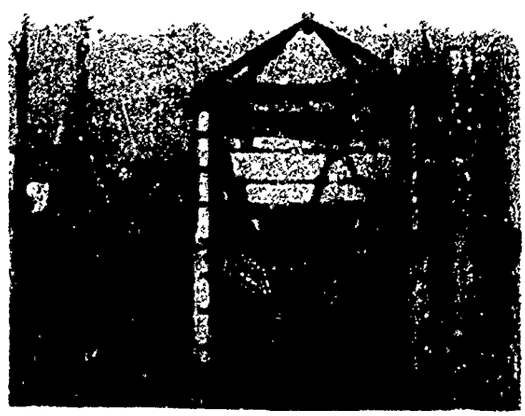

Cargo Stops
Time: .113 sec.

Figure 19. Test 14 Sequence Photos.

Load-Limited Inextensible Net (No. 14)

Drop height - 6 ft. free fall

Maximum relative cargo displacement - 10 in.

Stopping distance of cage - 6 in.

Maximum cage acceleration - 23.7G

Maximum cargo acceleration - 22.0G

Mean cargo acceleration - 8G

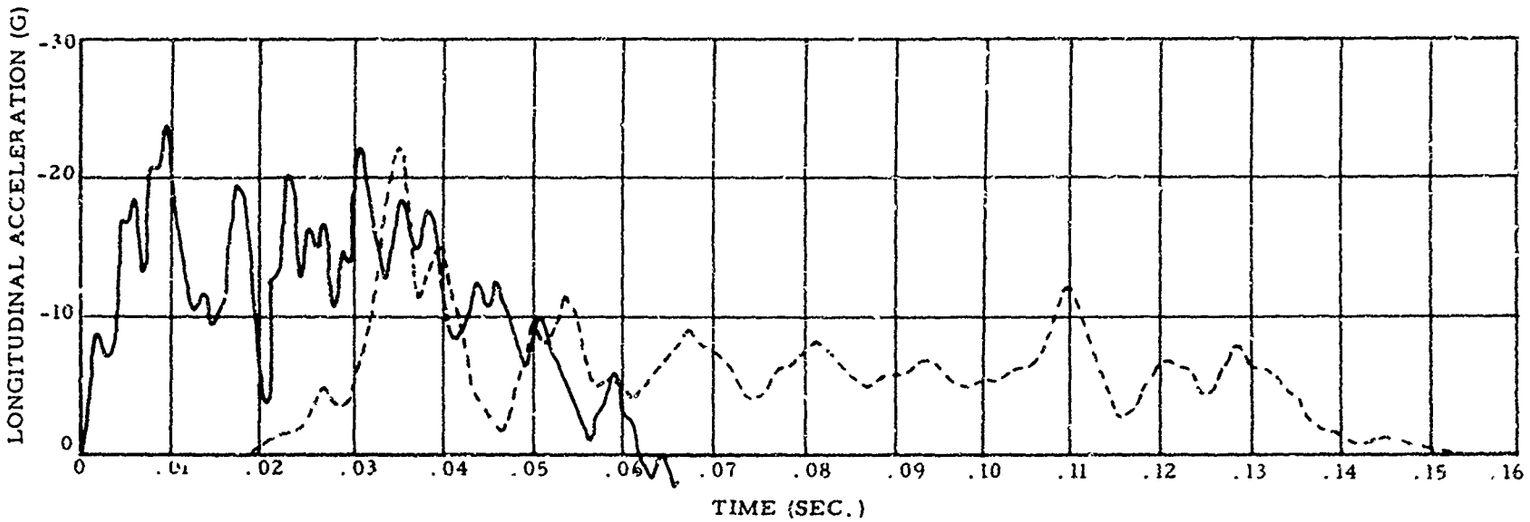

Figure 20. Drop Test 14 Data.

An additional experimental test of the inextensible linkage with load limiters is provided in the cargo experiment aboard the AvSER C-45 crash test (T-15). (See Figure 21). Load limiters were set for 15G and the aircraft crash pulse as measured by a structure-mounted accelerometer was as shown in Figure 22. Also shown are plots of load cells placed in series with the load limiters.

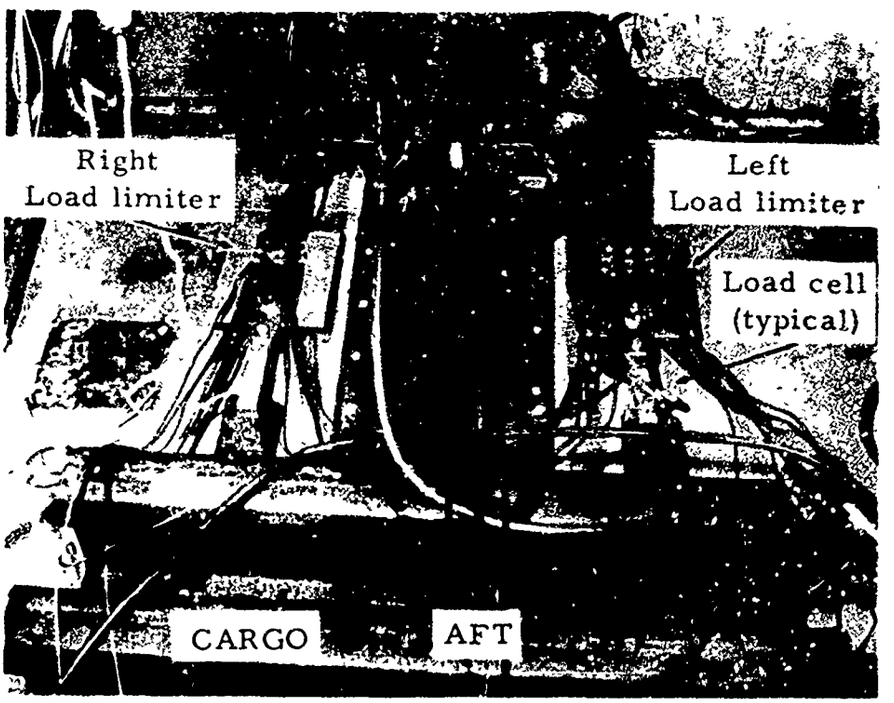

Figure 21. Cargo Experiment Aboard C-45.

AvSER Test T-15 Data

Load limiter stroke	1.5 inches (average)
Impact velocity	50 mph (approx.)
Impact angle	30° (approx.)

Cabin Floor Longitudinal Acceleration

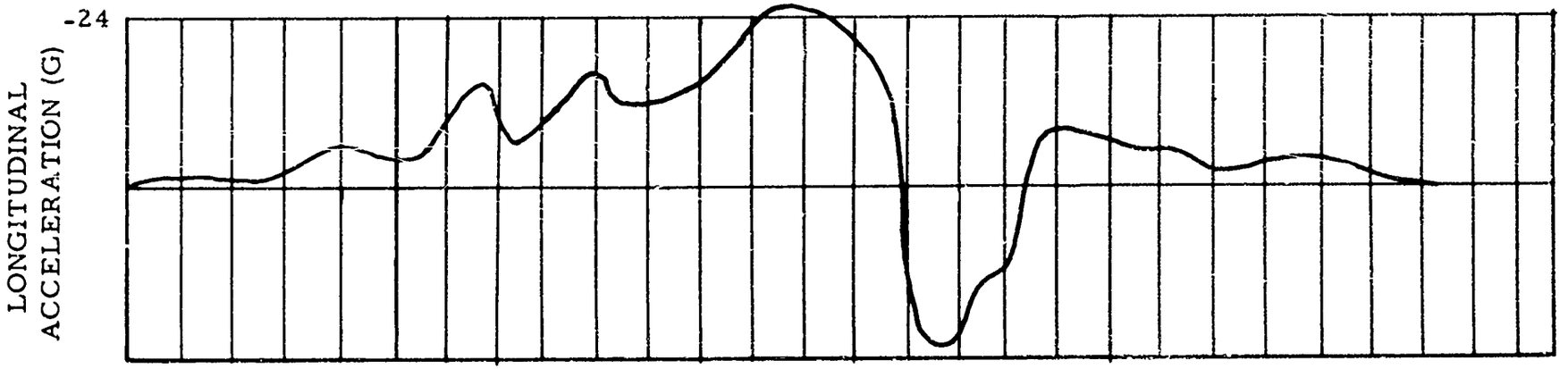

Left Hand Load-Limiter Force (Load Cell)

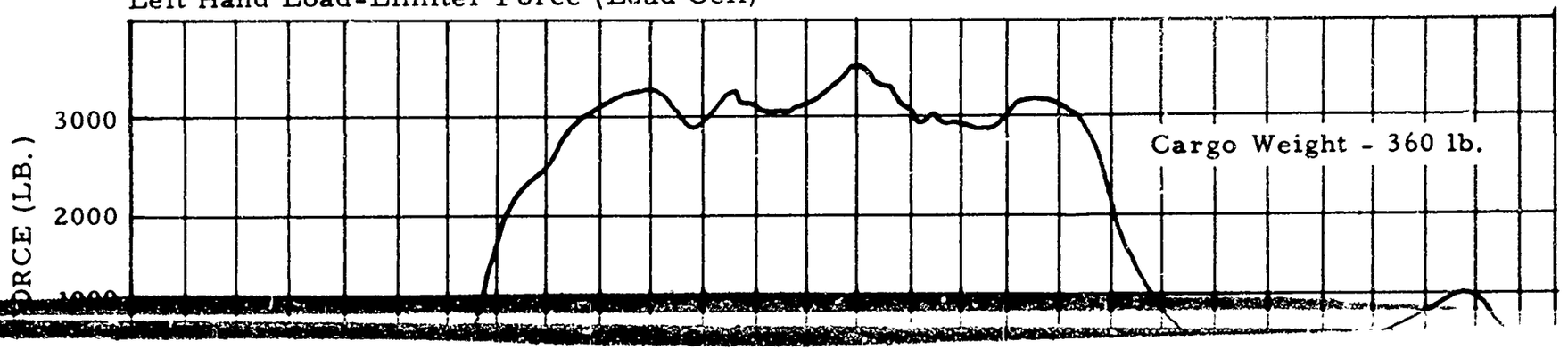

Left Hand Load-Limiter Force (Load Cell)

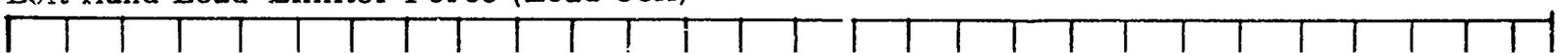

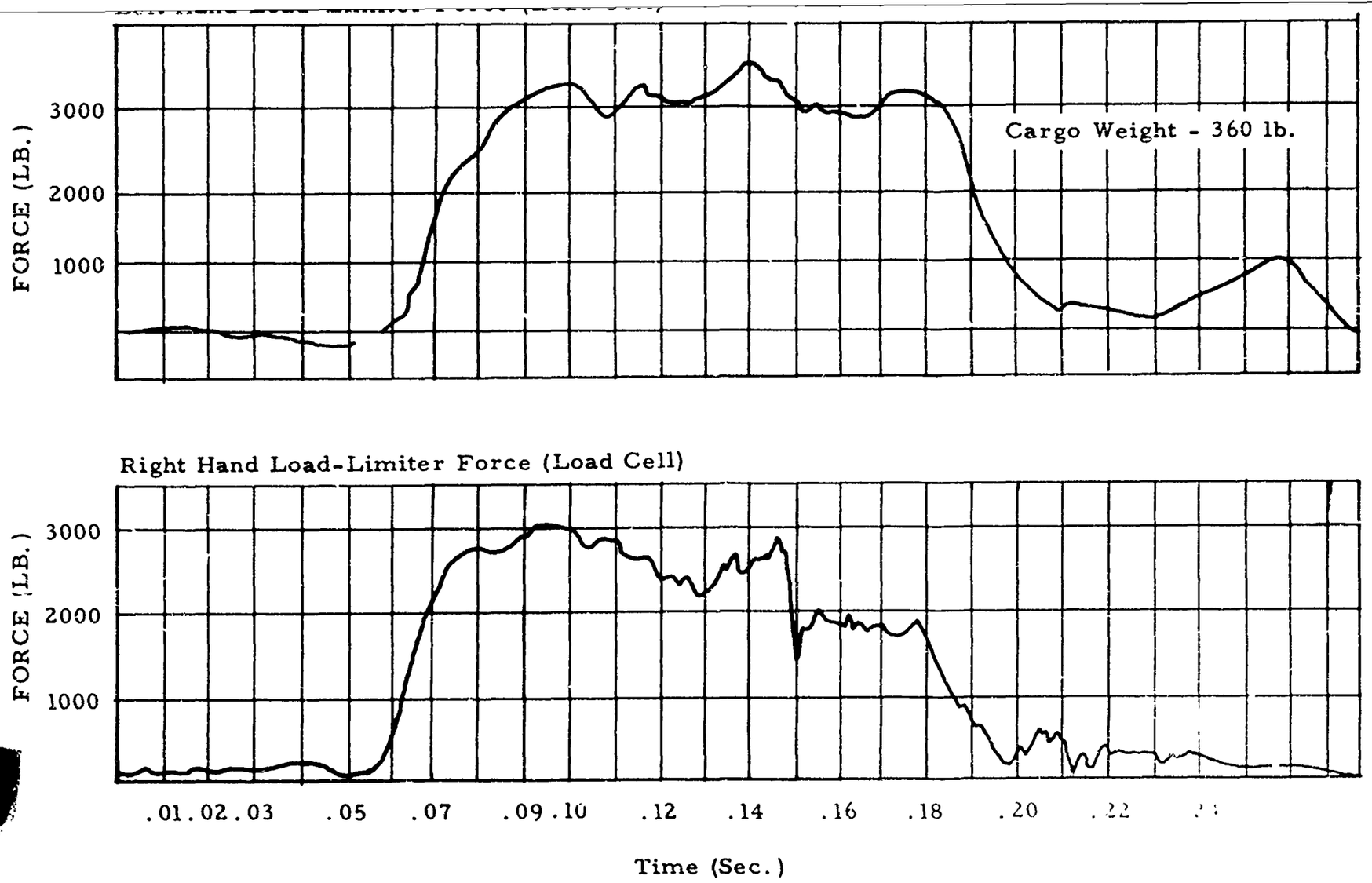

Figure 22. Accelerometer-Time and Force-Time Histories

The inextensible linkage load-limiter concept applied to the Caribou has been simulated on the computer for several settings of load limiter with the following results. A plot of load-limiter level versus cargo displacement appears in Figure 23. As with the extensible net, the required linkage strength depends upon the load-limiter level.

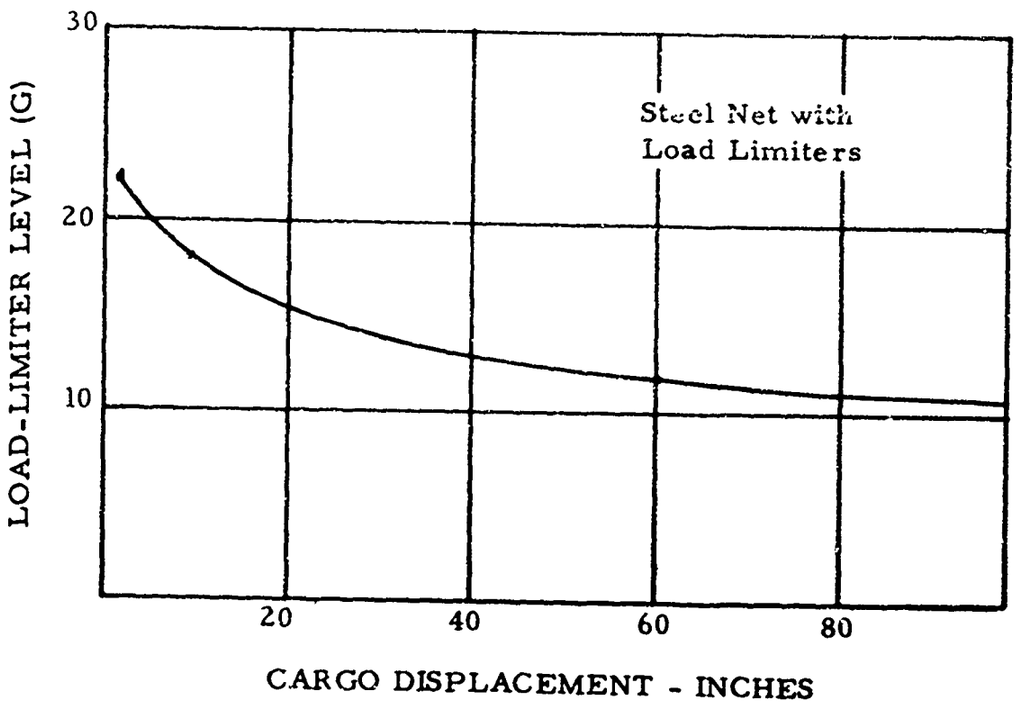

Figure 23. Load Limiter Level vs. Cargo Displacement. (Inextensible linkage)

It can be seen that cargo displacement again is significantly affected by modest changes in load-limiter level and in the same manner as with the extensible net.

DISCUSSION OF FIXED-WING AIRCRAFT CARGO RETENTION

SIMPLIFIED PULSE MODEL

A simplified pulse shape was assumed for the Caribou in the analysis of the various cargo restraint concepts discussed. A concern may arise as to the effect shape changes would have upon restraint system behavior. This has been investigated by means of computer simulation using a representative restraint system and appropriately modified input pulses from each of the three concepts discussed. Several modified pulse shapes, along with the standard pulse, are shown in Figure 24.

The effects of these modified pulse shapes upon cargo restraint system behavior is displayed in the comparison table on page 37.

It is seen that apart from pulse shape (the reduction in pulse duration with attendant increase in intensity) (F), no appreciable differences in retention system behavior occur. The proposed simplified shape is then a satisfactory model for design purposes. Also the inclusion of a "spike" superimposed upon the basic pulse shape (I) produces only slight differences. For a design criterion pulse, however, it is perhaps desirable to include such a spike, as the latter could produce serious effects upon a rigid restraint system of low ductility.

GENERAL COMPARISON OF CONCEPTS

Definite conclusions as to the relative suitability of the various design concepts explored would be premature. Selection of optimum materials, hardware details, and practical arrangements are yet to be evolved. It may be useful at this point, however, to indicate broad comparisons based upon tentative assumptions as to available materials, hardware, and possible practical arrangements.

For weight evaluation purposes, it is tentatively assumed that nylon has approximately 3 times the strength-to-weight ratio of a suitable high-strength steel, that hardware (exclusive of load limiters) is proportional to the load requirements and weighs approximately 6 times the nylon net proper, and that load limiter hardware, when included, adds an additional 40 percent to the hardware weight. From these assumptions the following comparison table results for the more practical arrangements among those investigated.

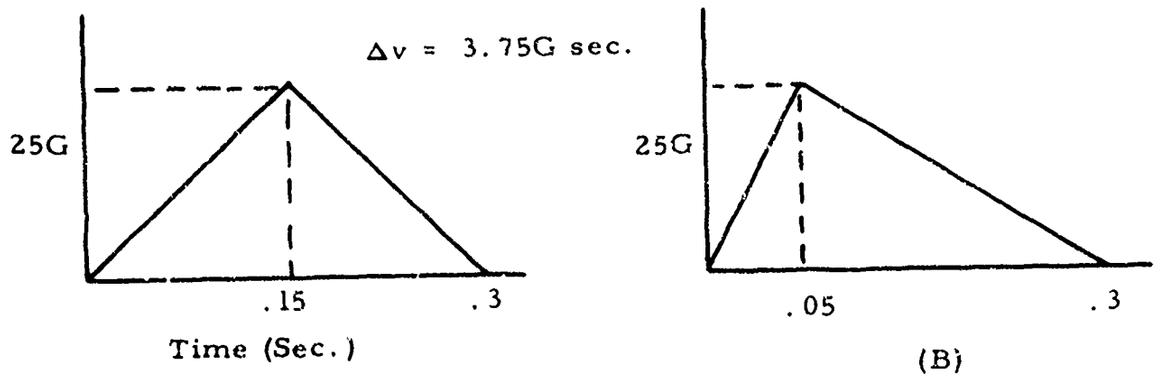

(A) Standard Pulse

(B)

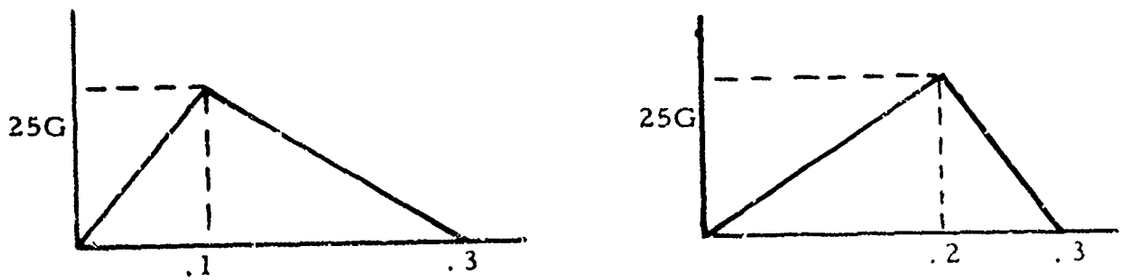

(C)

(D)

(E)

(F)

LONGITUDINAL ACCELERATION (G)

CELER

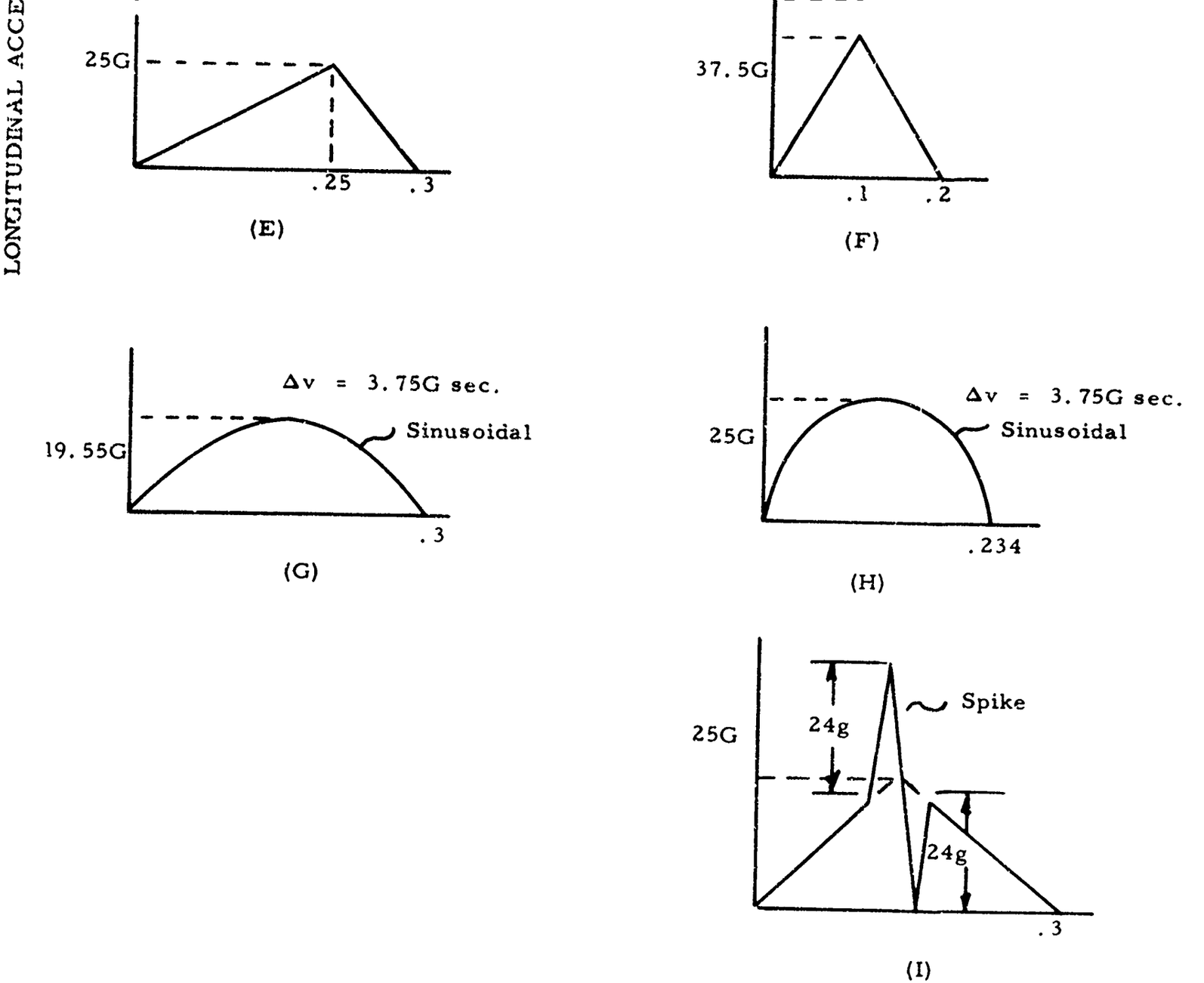

Figure 24. Standard Pulse Shape and Modified Pulse Shapes.

TABLE I

COMPARISON OF EFFECTS OF PULSE SHAPES

Pulse Shape		Nylon Net Without Load Limiters	Nylon Net With 25G Load Limiters	Steel Net With 18G Load Limiters
(A)  .3	Max. Rel. Displ. (in.)	20.40	51.02	9.27
	Stroke (in.)	0.0	32.16	9.27
	Max. Cargo Accel. (g)	63.5	25 0	18.0
	Max. Net Extension (in.)	20.40	18.8	0.0
(B)  .3	Max. Rel Displ. (in.)	22.62	54.69	11.64
	Stroke (in.)	0.0	35.77	11.64
	Max. Cargo Accel. (g)	87.5	25.0	18.0
	Max. Net Extension (in.)	22.62	18.8	0.0
(C)  .3	Max. Rel. Displ. (in.)	22.05	55.46	10.50
	Stroke (in.)	0.0	36.40	10.50
	Max. Cargo Accel. (g)	80.0	25.0	18.0
	Max. Net Extension (in.)	22.05	18.8	0.0
(D)  .3	Max. Rel. Displ. (in.)	18.98	42.99	7.91
	Stroke (in.)	0.0	23.97	7.91
	Max. Cargo Accel. (g)	51.0	25.0	18.0
	Max. Net Extension (in.)	18.98	18.8	0.0
(E)  .3	Max. Rel. Displ. (in.)	17.95	32.74	6.31
	Stroke (in.)	0.0	13.69	6.31
	Max. Cargo Accel. (g)	43.7	25.0	18.0
	Max. Net Extension (in.)	17.95	18.8	0.0
(F)  .2	Max. Rel Displ. (in.)	25.12	84.36	40.15
	Stroke (in.)	0.0	65.53	40.15
	Max. Cargo Accel. (g)	118.0	25.0	18.0
	Max. Net Extension (in.)	25.12	18.8	0.0
(G) 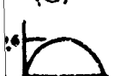 .3	Max. Rel. Displ. (in.)	20.13	43.75	1.94
	Stroke (in.)	0.0	24.83	1.94
	Max. Cargo Accel. (g)	61.0	25.0	18.0
	Max. Net Extension (in.)	20.13	18.8	0.0
(H)  .2	Max. Rel. Displ. (in.)	22.37	64.65	18.58
	Stroke (in.)	0.0	45.82	18.58
	Max. Cargo Accel. (g)	84.5	25.0	18.0
	Max. Net Extension (in.)	22.37	18.8	0.0
(I)  .3	Max. Rel. Displ. (in.)	21.58	52.88	11.12
	Stroke (in.)	0.0	34.01	11.12
	Max. Cargo Accel. (g)	75.6	25.0	18.0
	Max. Net Extension (in.)	21.58	18.8	0.0

TABLE II

WEIGHTS AND DISPLACEMENTS FOR SELECTED RESTRAINT SYSTEMS*

System	Weights (lb.) Net	Restraint Hardware	Limiter Hardware	Total	Displacement (inches)
160 KIP Nylon Net without load limiters	9	58	0	67	20.4
107 KIP Nylon Net with 25G load limiters	6	37	15	58	51.0
Inextensible Net with 12G load limiters	9	18	8	35	60.0
Inextensible Net with 18G load limiters	14	27	12	53	9.3

*Estimated weights and displacements are based on restraining a 2600-pound load when subjected to the simplified crash pulse previously described.

Caution should be used in interpreting the above comparison table as material selection and weight assumptions are based upon incomplete design knowledge. The comparison does demonstrate, however, that alternate design concepts are worthy of more detailed development.

DISCUSSION OF ROTARY-WING CARGO RESTRAINT

A review of helicopter dro,. ests designed to simulate typical helicopter accidents (Ref. 1, 2, and ( ) shows the vertical acceleration, in general, to be greater than twice the longitudinal acceleration during the principal impact. Thus, if a coefficient of friction between cargo and floor were as great as .5, little or no cargo displacement would occur. The presence of flight load cargo restraint would lend additional support against cargo displacement during the crash sequence. Thus, there is the strong possibility that flight load restraint, together with floor friction, is sufficient for crew protection during a typical survivable helicopter crash. However, some uncertainties do exist. The vertical and longitudinal accelerations may not be entirely synchronized. Also, although tests conducted so far have shown smaller longitudinal accelerations than vertical, a crash into softer terrain might admit greater longitudinal forces from the plowing action. Finally, for stacked cargo, tumbling action rather than sliding could occur with friction offering little assistance. In view of these uncertainties, an experimental program to confirm the adequa y of flight load tiedown is recommended.

If load limiters were employed, cargo displacement would be governed by the input acceleration pulse and the load-limiter level (as with the fixed-wing aircraft). Employing a load-limiter level at the flight load requirement of 4G, ignoring assistance from floor friction and using the longitudinal acceleration-time data from the H-25 helicopter crash test (AvSER Test No. 1, Ref. 1), a computer simulation leads to a load-limiter stroke of 11.7 inches. This appears to be acceptable and would indicate that moderate load-limited cargo retention would prove an adequate solution to helicopter cargo tiedown. Verification by drop tests and helicopter tests is considered desirable, with the strong possibility that experimental evidence may even admit the reduced requirement of only flight load restraint.

MATERIAL SELECTION AND DESIGN TECHNIQUES

An important aspect of cargo restraint design involves the selection of suitable materials and hardware to provide effective cargo restraint for a minimum cost in weight. Several observations and considerations are offered here as a result of analyses and tests performed:

1. Nylon (also dacron) nets or straps possess a high strength-to-weight ratio and as such would appear to be attractive restraint material. The load-elongation curve for nylon, however, is non-linear with increasing modulus. This leads to significant dynamic overshoot which offsets the high ultimate strength of the nylon by subjecting the system to greater decelerative forces than direct floor decelerations would produce. As noted earlier in the report, the use of load limiters with a nylon-type restraint serves only to exchange this higher strength requirement for large cargo displacements. Space limitations may not admit such an exchange.

2. High-strength steel, although possessing a lower ultimate strength-to-weight ratio than nylon, offers the distinct advantage of being comparatively inextensible. Hence, dynamic overshoot is absent, which results in lower strength requirements and/or smaller cargo displacements when using load-limiter devices. Considerable promise is offered by recently developed ultra-high-strength steels, with strength-to-weight ratios approaching those of the synthetic fibers. The use of steel foil was explored as a possible inextensible (yet flexible) membrane to restrain cargo. However, the foil was found to be highly sensitive to edge effects or other geometric discontinuities. Tearing was readily produced and easily propagated.

   Nets or restraint linkages employing high-strength steel wire or high-strength cable offer most promise when used with load-limiter devices.

3. The application of load limiters in attenuating the energy associated with peak pulses has been demonstrated and discussed in this report. The problem of efficient design of such devices still remains.

   Several alternate methods of inelastic energy absorption are available for use in load limiters, four of which are listed below:

a. Relative movement between surfaces with dry friction present.
b. Tearing action of tubes or thin plates.
c. Plastic deformation of a tube to change its diameter (a drawing operation or a plastic expansion).
d. Flexural plastic stress reversals of a strap or wire.

The use of dry friction suffers from a lack of controlability which is vital to a good load-limiter device. Either tearing action (b) or one-time plastic deformation (c) would be less efficient (on a per-weight basis) than plastic stress reversals (d), as the latter employs the same deformable material for several repetitions of energy dissipation action.

The stress-reversal technique is therefore to be preferred and may be accomplished practically by pulling an interwoven wire or strap through holes in a plate or around fixed posts so as to cause alternately plastic flexure and counter flexure.

4. In order to adapt a cargo restraint system to existing tiedown points on the Caribou cargo floor, attention must be given to distributing the load equally to several tiedown points. One means of accomplishing this for a load-limited system would be to employ load limiters at each tiedown location. Thus, the load limiters would perform two functions - attenuate peak pulse energy and ensure equal distribution of force to tiedown points.

An alternative arrangement would employ a minimum of load limiters in the main line of restraint force transmission together with "load-equalizers" at each tiedown location. The load-equalizer is similar to a load limiter except that it would be designed for a much smaller stroke, as energy absorption is not the purpose. The stroke would be sufficient to cause a redistribution of force from an otherwise overloaded tiedown ring to other rings. With this single function, load-equalizer devices could be made much lighter than load limiters.

Further study and development of an integrated cargo system should include an investigation of practical features of each of the arrangements discussed above.

REFERENCES

1. Turnbow, J. W., U. S. Army H-25 Helicopter Drop Test, 22 October 1960, Technical Report, TREC Technical Report 60-76, AvCIR-2-TR-125, Aviation Crash Injury Research, Phoenix, Arizona, 15 March 1961.

2. Carroll, D. F. and Peterson, R. G., 1961 Helicopter Drop Test Program Conducted for the Flight Safety Foundation, Inc., No. AER-F2R-13572 Vought Aeronautics, Dallas, Texas, Sept. 1961.

3. Preston, G. Merritt and Pesman, Gerald J., Accelerations In Transport - Airplane Crashes, NACA TN4158, Lewis Flight Propulsion Laboratory, Cleveland, Ohio, February 1958.

4. Eiband, A. Martin, Simpkinson, Scott H., and Black, Dugald O., Accelerations and Passenger Harness Loads Measured in Full-Scale Light Airplane Crashes, NACA TN2991, Lewis Flight Propulsion Laboratory, Cleveland, Ohio, August 1953.

5. Acker, Loren W., Black, Dugald O., and Moser, Jacob C., Accelerations in Fighter Airplane Crashes, NACA RM E 57G11, Lewis Flight Propulsion Laboratory, Cleveland, Ohio, Nov. 1957.

6. NACA Conference on Airplane Crash-Impact Loads, Crash Injuries and Principles of Seat Design for Crashworthiness, Lewis Flight Propulsion Laboratory, Cleveland, Ohio, April 1956.

7. Model Specification AC-1 DH Caribou, AEROC 4b. 1. G.2, Issue 2. Revision 1, U. S. Army, The DeHavilland Aircraft of Canada, Ltd., December 1959.

8. Reed, W. H. and Carroll, D. F., CH-21A Helicopter Airframe Deformation Under A Dynamic Crash Condition, TRECOM 63-77, Aviation Safety Engineering and Research, Phoenix, Arizona, January 1964.

9. Detail Specification For The Model YHC-1B Helicopter Transport, 114-X-01, Vertol Aircraft Corporation, Morton, Pennsylvania, October 1959.

REFERENCES (Contd.)

10. Bibliography Of Impact Acceleration Literature (Project SIAT) TRECOM 63-31B, Flight Safety Foundation, Inc., New York, New York, June 1963.

11. Bibliography of AvSER Reports, Aviation Safety Engineering and Research, Phoenix, Arizona, May 1964.

DISTRIBUTION

US Army Materiel Command	2
US Army Mobility Command	2
US Army Aviation Materiel Command	5
Chief of R&D, D/A	3
US Army Aviation Materiel Laboratories	19
USAAML Liaison Officer, US Army R&D Group (Europe)	1
US Army Natick Laboratories	1
US Army Engineer R&D Laboratories	2
US Army Limited War Laboratory	1
US Army Human Engineering Laboratories	2
Army Research Office-Durham	1
US Army Test and Evaluation Command	1
US Army Research Support Group	1
US Army Medical R&D Command	1
US Army Combat Developments Command, Fort Belvoir	1
US Army Combat Developments Command Aviation Agency	2
US Army Combat Developments Command Transportation Agency	1
US Army Combat Developments Command Quartermaster Agency	1
US Army Combat Developments Command Experimentation Command	1
US Army Transportation School	1
US Army Aviation School	1
US Army Quartermaster School	1
Deputy Chief of Staff for Logistics, D/A	1
US Army Transportation Center and Fort Eustis	1
US Army Aviation Test Board	1
TC Liaison Officer, US Army Airborne, Electronics and Special Warfare Board	1
US Army Aviation Test Activity	1
US Army Transportation Engineering Agency	1
US Army General Equipment Test Activity	1
Air Force Flight Dynamics Laboratory, Wright-Patterson AFB	1
Air Force Flight Test Center, Edwards AFB	1
Chief of Naval Research	1
US Naval Air Station, Patuxent River	1
Marine Corps Liaison Officer, US Army Transportation School	1
NASA-LRC, Langley Station	1
NASA Representative, Scientific and Technical Information Facility	2
National Aviation Facilities Experimental Center	1
Defense Documentation Center	20

APPENDIX I. CRASH PULSE SIMULATOR

The pulse simulation computer program is designed to develop a longitudinal acceleration-time curve for a given aircraft under simplified (and idealized) accident conditions.

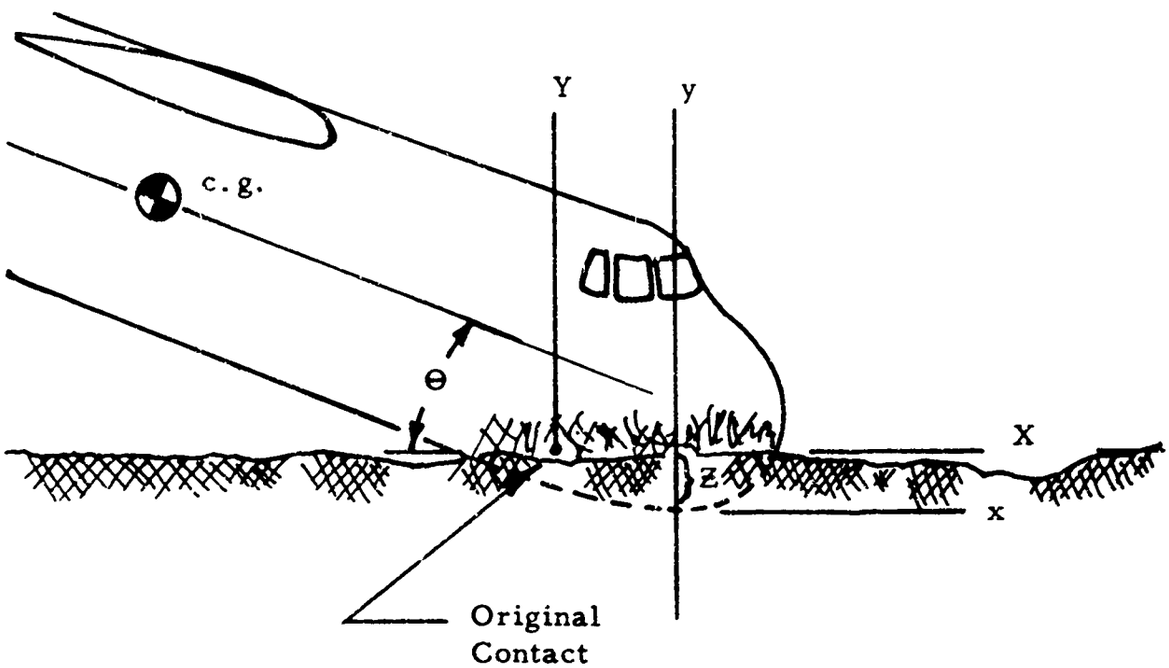

NOMENCLATURE

x,y ... Coordinates of aircraft center of gravity from the x,y axis system

X,Y ... Coordinates of aircraft center of gravity from the original point of contact

Z ... Crush distance of aircraft hull measured along the y axis

Δ ... The change in a quantity corresponding to an increment of time, Δ t

k ... Radius of gyration of the aircraft

θ ... Angle between the longitudinal axis of the aircraft and the plane of contact

ω ... Angular velocity, $\frac{d\theta}{dt}$

α ... Angular acceleration, $\frac{d^2\theta}{dt^2}$

μ ... Coefficient of plowing

V_x ... Velocity of the center of gravity in the x direction

V_y ... Velocity of the center of gravity in the y direction

V ... Longitudinal velocity of the center of gravity

Ax ... Acceleration of the center of gravity in the x direction

Ay ... Acceleration of the center of gravity in the y direction

A ... Longitudinal acceleration of the center of gravity

m ... Mass of the aircraft

PROGRAM INPUT

The program accepts as input:

Geometric contour constants ..... A_1, A_2, A_3, A_4, B_1, B_2, B_3, B_4

Structure and ground resistance constants ..... C_1, C_2, C_3, C_4,

D_1, D_2, D_3, D_4, F_1, F_2, F_3, F_4

Coefficient-of-plowing constants ..... E_1, E_2, E_3, E_4

Impact velocity V

Impact angle ..... θ_o

Time increment ..... Δt

Radius of gyration ..... k

Mass of aircraft ..... m

PROGRAM OUTPUT

For each time increment the following quantities are displayed: elapsed time; longitudinal acceleration; X and Y components of acceleration, velocity, and displacement; angular acceleration, velocity, and rotation.

MATHEMATICAL MODEL

The geometric contour of the fuselage is expressed in terms of the angle θ. Specifically, the coordinates (x,y) of the aircraft center of gravity with respect to a contour axis system shown (x-axis tangential to the contour) are assumed to be polynomials in θ:

$$x = A_1 + A_2\theta + A_3\theta^2 + A_4\theta^3$$

$$y = B_1 + B_2\theta + B_3\theta^2 + B_4\theta^3$$

Forces acting upon the aircraft in the x and y directions are determined by the interference of the original contour with the ground surface (implying both penetration of soil and crushing of aircraft structure). A nonlinear relationship is assumed for penetration and a linear relationship for a spring-back phase. Thus, the acceleration components for penetration are:

$$Ay = H_1Z + H_2Z^2,$$

$$Ax = \mu Ay,$$

and for the spring-back phase the acceleration increment is:

$$Ay = H_3\Delta Z.$$

The resistance constants H_1, H_2, and H_3, as well as the coefficient of plowing, μ are functions of the angle θ:

$$H_1 = C_1 + C_2\theta + C_3\theta^2 + C_4\theta^3$$

$$H_2 = D_1 + D_2\theta + D_3\theta^2 + D_4\theta^3$$

$$H_3 = F_1 + F_2\theta + F_3\theta^2 + F_4\theta^3$$

$$\mu = E_1 + E_2\theta + E_3\theta^2 + E_4\theta^3.$$

Numeric integration is performed for each time increment to obtain velocities and displacements (for both translational and rotational motions), thus:

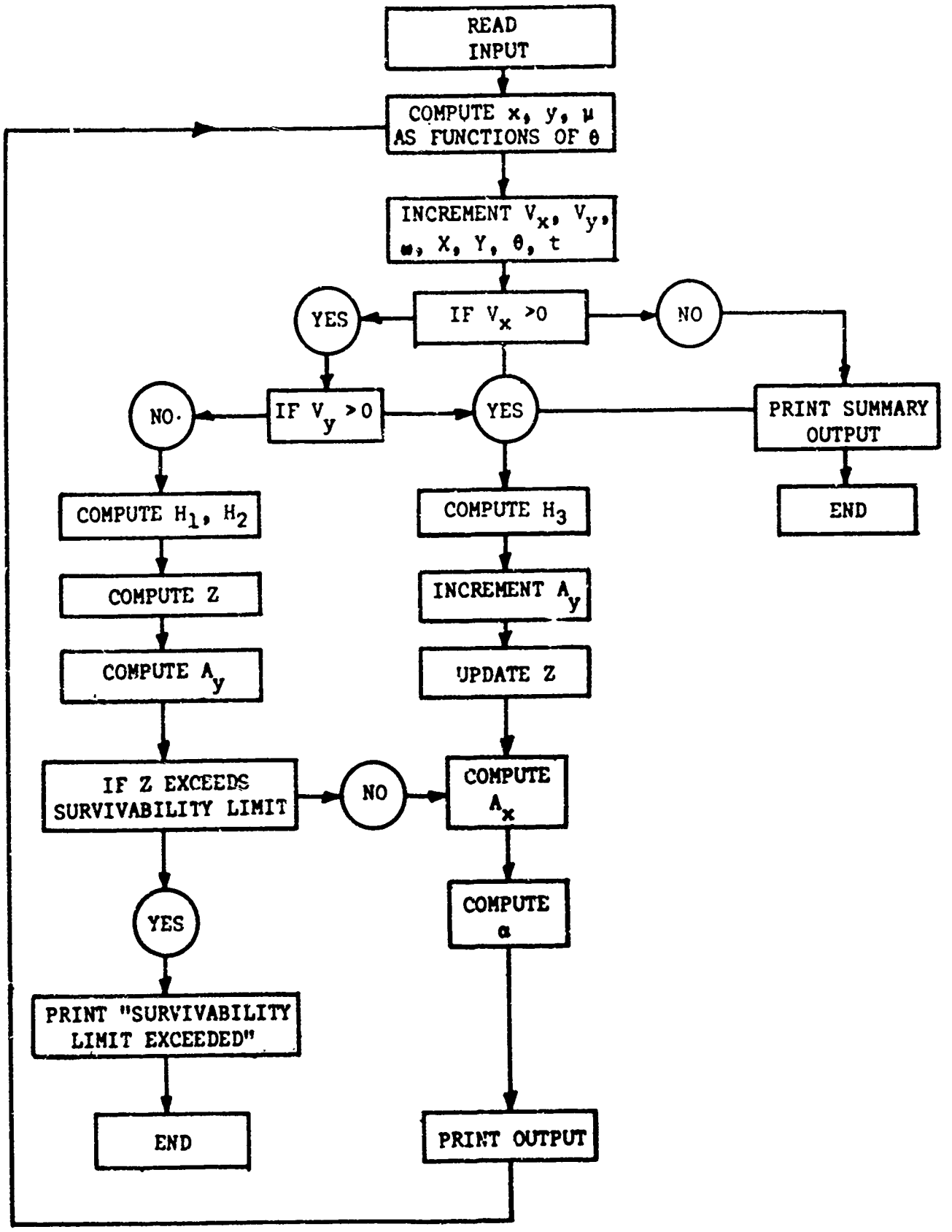

Figure 25 . General Flow Chart for Crash Pulse Simulation.

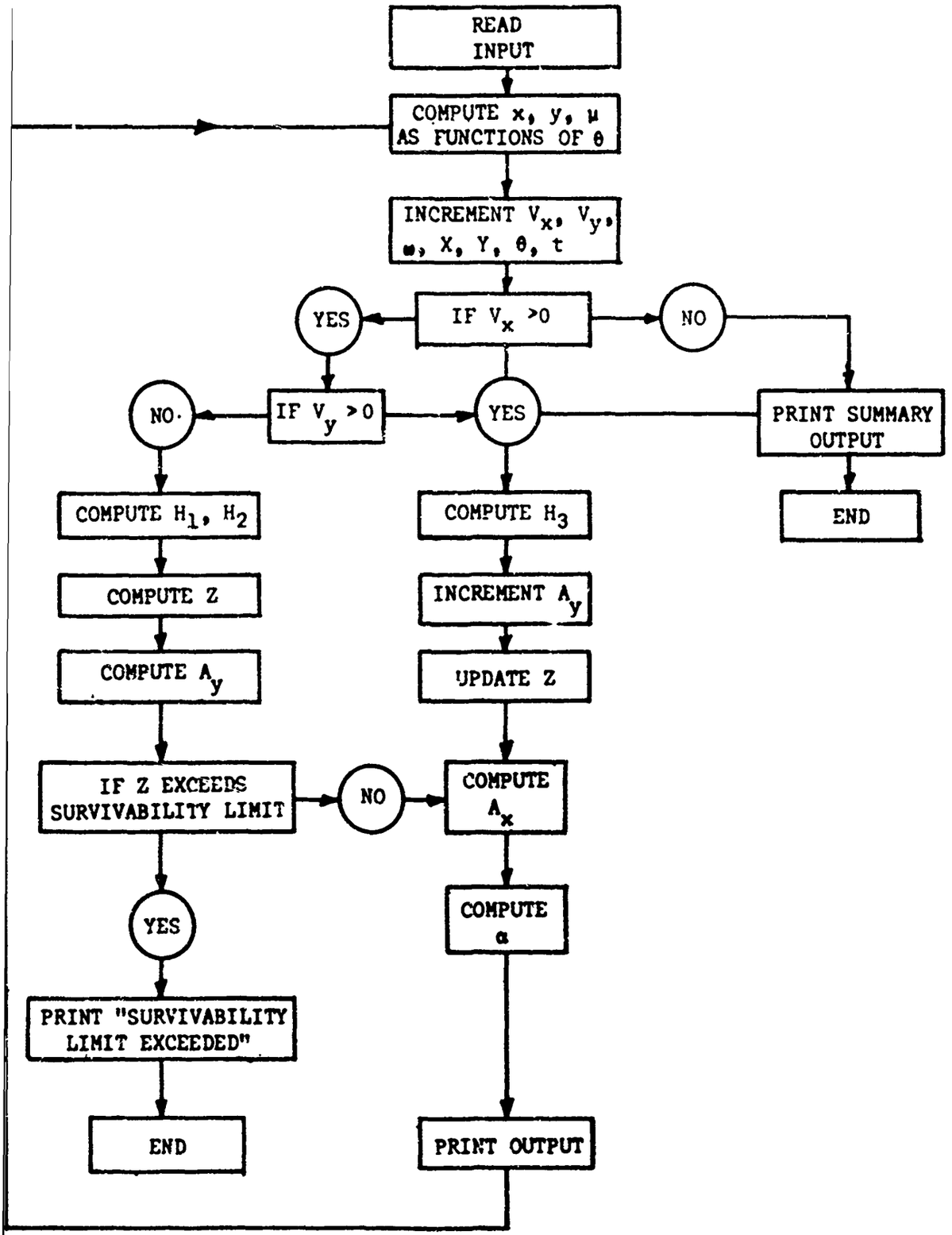

Figure 25 . General Flow Chart for Crash Pulse Simulation.

APPENDIX II. DROP TEST SETUP

TEST APPARATUS

The drop test equipment is shown in Figure 26. The descriptions of the various items are as follows:

EQUIPMENT WEIGHTS

Drop Frame	330 lb
Intermediate Slide Frame	35 lb
Simulated Cargo Weight	155 lb
Total.	520 lb

LOAD LIMITERS

See sketch ..... load-limiter detail. (G-level regulated by hold spacing.)

CARGO RELEASE

See sketch ..... cargo release detail.

Cargo releases at 200-lb force.

HOLDDOWN CABLE

Small cables suspended over cargo to limit slack during free fall.

HONEYCOMB PAD

No. blocks per test	5

Block Dimensions

Thickness.	3 in.
Area	216 sq. in.
Type	3/8 in. cell, nonimpregnated paper honeycomb
Manufacturer	Hexcell

NOTE: Prior to each test, the top and bottom blocks were precrushed approximately 1/4 in.

INSTRUMENTATION

Cage Accelerometer	± 200 G, No. A5-200-350 Statham Instruments Corp.
Cargo Accelerometer	± 50 G, No. A5-50-350 Statham Instruments Corp.
Oscillograph	No. 5-124 Consolidated Electrodynamics Corp.

CAMERA

Type	Photo-Sonics 1-B, 16mm
Frame Rate	Approximately 500 fps
Manufacturer	Photo-Sonics, Inc.

TEST PROCEDURE

1. The load limiters (or rigid linkages) (5) appropriate for the test were placed into position shown in sketch.

2. The simulated cargo weight (3) was raised into position and was supported by a cable (12).

3. The net (4) to be tested was positioned in the slide frame (2).

4. Hold down cables (9) were placed over the cargo to prevent the support cable (12) from becoming slack during free fall.

5. The top and bottom blocks of the honeycomb pad were precrushed and the pad (10) was centered under the drop frame base.

6. The test apparatus was raised to a predetermined height above the honeycomb pad.

7. The accelerometer output signal was calibrated and the oscillograph paper speed was set to 64 in. per second.

8. When the high-speed recording camera was brought up to speed, the electric release hook was actuated, allowing the drop test to proceed.

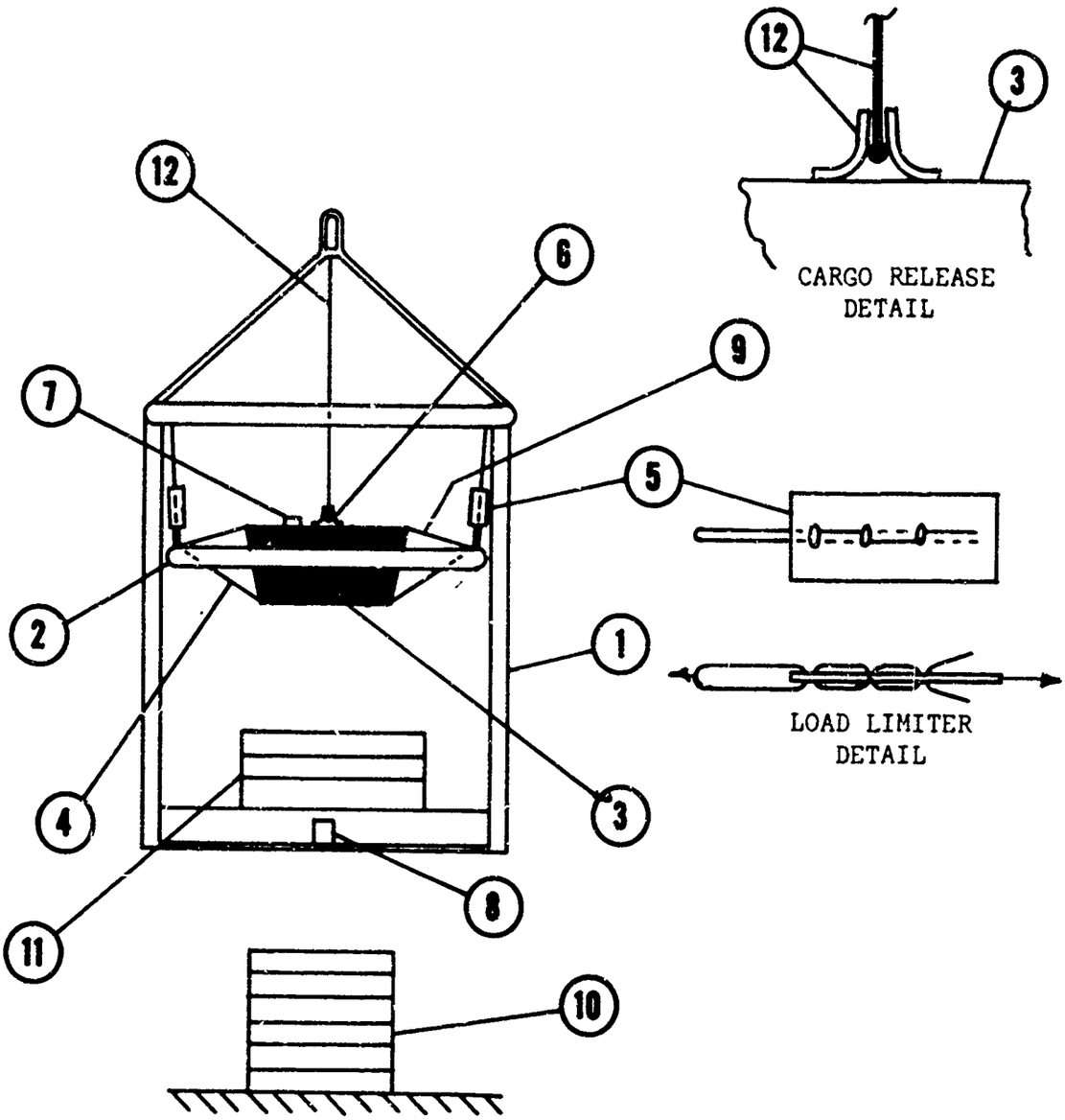

DROP ASSEMBLY

1. DROP FRAME
2. INTERMEDIATE SLIDE FRAME
3. CARGO
4. NET
5. LOAD LIMITER
6. CARGO RELEASE
7. CARGO ACCELEROMETER
8. CAGE ACCELEROMETER
9. HOLD DOWN CABLE
10. PAPER HONEYCOMB PAD
11. HONEYCOMB CUSHION MATERIAL
12. CARGO SUPPORT CABLE AND RELEASE

NOT SHOWN: HIGH-SPEED CAMERA
ELECTRICALLY CONTROLLED RELEASE HOOK
RECORDING OSCILLOGRAPH

Figure 26. Drop Test Setup.

APPENDIX III. CARGO RESTRAINT SYSTEM SIMULATOR

The computer program to simulate cargo restraint systems is designed to obtain the dynamic response of a cargo retention system to an applied aircraft acceleration pulse.

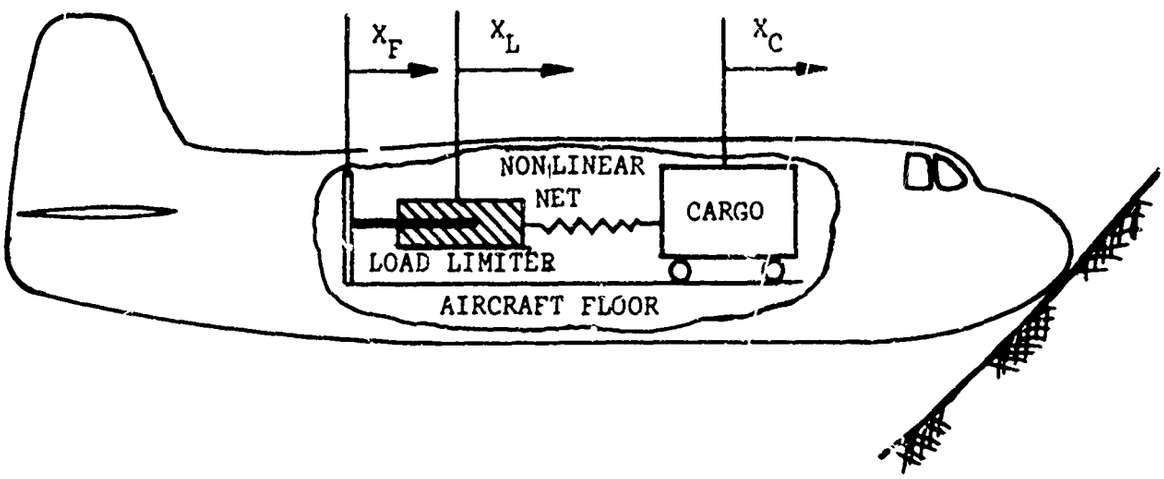

NOMENCLATURE

X_F ... Displacement of aircraft cargo floor

X_L ... Displacement of load limiter

X_C ... Displacement of cargo

A,B,C . Elastic constants for (nonlinear) net

δ ... Deflection of cargo net

F_n ... Force upon cargo net

V_F ... Velocity of cargo

V_C ... Velocity of cargo

A_F ... Acceleration of cargo floor

A_C ... Acceleration of cargo

S ... Stroke of load limiter

t ... Time (from beginning of pulse)

t_{slack} ... Slack time, i.e., time for cargo to achieve contact with net

Δt ... Time increment

m_c ... Cargo mass

INPUT

The program accepts as input:

Force-displacement constants for extensible net (if applicable)	A,B,C
Weight of cargo	W
Load-limiter level	G_L
Impact velocity	V
Cargo "Slack time"	t_{slack}
Acceleration of aircraft at time t_i	G_i i = 1,N
Indicator for inextensible net (if applicable)	

OUTPUT

The program output includes floor displacement, limiter stroke, cargo displacement, aircraft velocity, cargo velocity, and aircraft acceleration at regular time intervals.

MATHEMATICAL MODEL AND RELATIONSHIPS EMPLOYED

Referring to the foregoing (sketch and nomenclature), the force required to deflect the nonlinear net on amount δ is expressable as a cubic in δ:

$$F_n = A\delta + B\delta^2 + C\delta^3.$$

Then for the cargo mass m_c, the consequent acceleration is:

$$A_c = \frac{F_n}{m_c} .$$

The cargo floor acceleration is obtainable by means of interpolation from input acceleration time data.

Finite difference integration may be employed to increment velocities:

$$V_{F_{i+1}} = V_{F_i} + A_{F_i} \Delta t$$

$$V_{C_{i+1}} = V_{C_i} + A_{C_i} \Delta t.$$

Displacement in turn may be incremented by finite differences:

$$X_{F_{i+1}} = X_{F_i} + V_{F_i} \Delta t$$

$$X_{C_{i+1}} = X_{C_i} + V_{C_i} \Delta t.$$

The stroke of load limiters is incremented only when the load-limiter slip load is reached. Then the increment in stroke is obtained from the relative velocity between the cargo and floor:

$$S_{i+1} = S_i + (V_{C_i} - V_{F_i}) \Delta t.$$

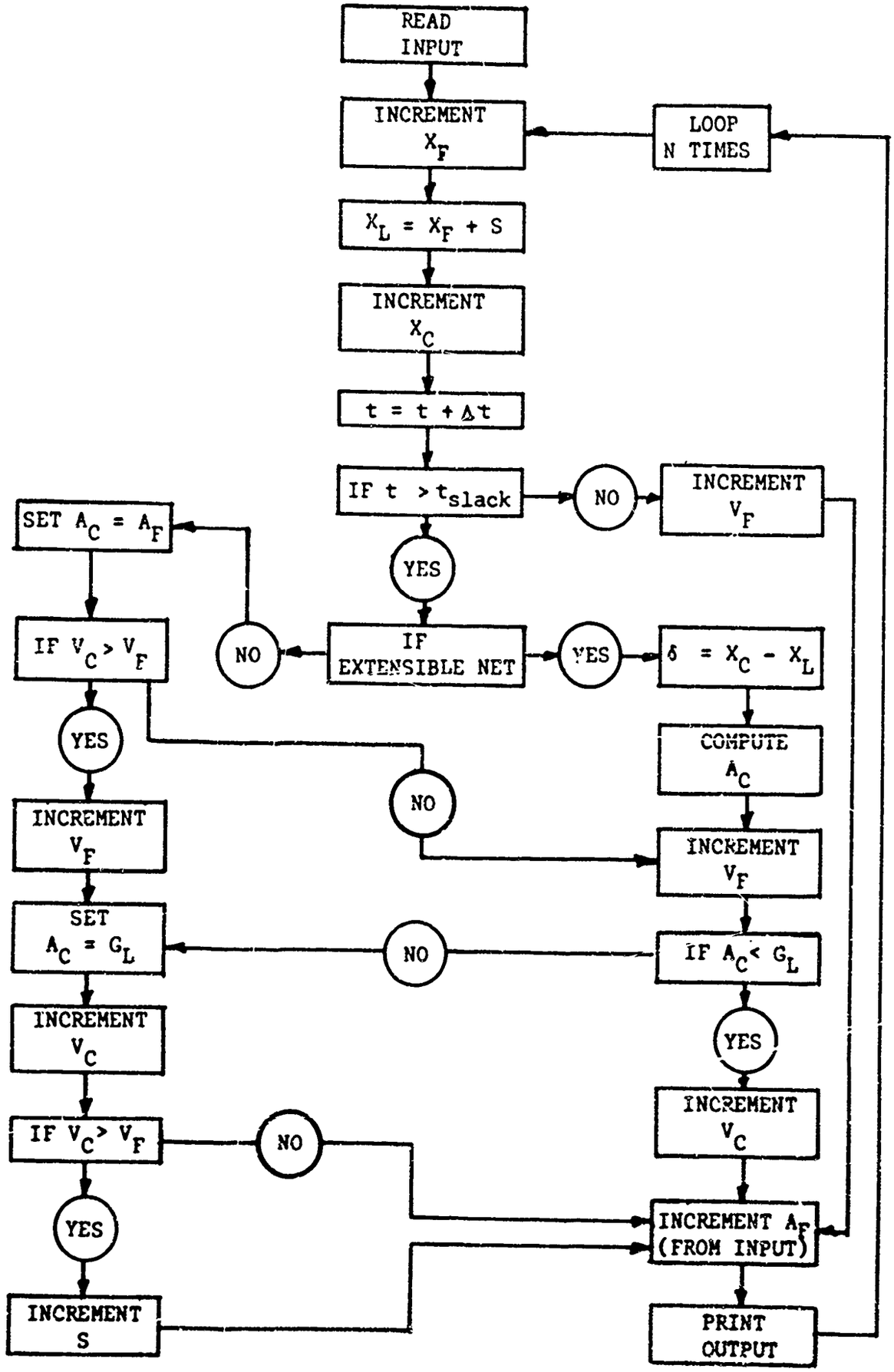

Figure 27. General Flow Chart for Cargo Restraint System Simulator.